

Kristina A. Dahl · Anthony J. Broccoli  
Ronald J. Stouffer

## Assessing the role of North Atlantic freshwater forcing in millennial scale climate variability: a tropical Atlantic perspective

Received: 15 March 2004 / Accepted: 5 November 2004 / Published online: 22 February 2005  
© Springer-Verlag 2005

**Abstract** This study analyzes a three-member ensemble of experiments, in which 0.1 Sv of freshwater was applied to the North Atlantic for 100 years in order to address the potential for large freshwater inputs in the North Atlantic to drive abrupt climate change. The model used is the GFDL R30 coupled ocean–atmosphere general circulation model. We focus in particular on the effects of this forcing on the tropical Atlantic region, which has been studied extensively by paleoclimatologists. In response to the freshwater forcing, North Atlantic meridional overturning circulation is reduced to roughly 40% by the end of the 100 year freshwater pulse. Consequently, the North Atlantic region cools by up to 8°C. The extreme cooling of the North Atlantic increases the pole-to-equator temperature gradient and requires more heat be provided to the high latitude Atlantic from the tropical Atlantic. To accommodate the increased heat requirement, the ITCZ shifts southward to allow for greater heat transport across the equator. Accompanying this southward ITCZ shift, the Northeast trade winds strengthen and precipitation patterns throughout the tropical Atlantic are altered. Specifically, precipitation in Northeast Brazil increases, and precipitation in Africa decreases slightly. In addition, we find that surface air temperatures warm over the tropical Atlantic and over Africa, but cool over

northern South America. Sea-surface temperatures in the tropical Atlantic warm slightly with larger warm anomalies developing in the thermocline. These responses are robust for each member of the ensemble, and have now been identified by a number of freshwater forcing studies using coupled OAGCMs. The model responses to freshwater forcing are generally smaller in magnitude, but have the same direction, as paleoclimate data from the Younger Dryas suggest. In certain cases, however, the model responses and the paleoclimate data directly contradict one another. Discrepancies between the model simulations and the paleoclimate data could be due to a number of factors, including inaccuracies in the freshwater forcing, inappropriate boundary conditions, and uncertainties in the interpretation of the paleoclimate data. Despite these discrepancies, it is clear from our results that abrupt climate changes in the high latitude North Atlantic have the potential to significantly impact tropical climate. This warrants further model experimentation into the role of freshwater forcing in driving climate change.

---

K. A. Dahl (✉)  
Massachusetts Institute of Technology/  
Woods Hole Oceanographic Institution Joint Program,  
WHOI MS #22, Woods Hole, MA 02543, USA  
E-mail: kdahl@whoi.edu  
Tel.: +1-508-2892853  
Fax: +1-508-4572187

A. J. Broccoli  
Department of Environmental Sciences,  
Rutgers University, 14 College Farm Road,  
New Brunswick, NJ 08901, USA

R. J. Stouffer  
Geophysical Fluid Dynamics Laboratory, P.O. 308,  
Princeton, NJ 08542, USA

---

### 1 Introduction

This study examines the response of the tropical Atlantic to a freshwater input in the North Atlantic using a coupled ocean–atmosphere general circulation model. The motivation for performing freshwater forcing experiments such as this one stems from the hypothesis that millennial-scale climate changes are driven by rapid increases in freshwater input to the North Atlantic from the melting of continental ice sheets (Broecker et al. 1985, 1988). Such freshwater inputs may cause a density stratification of the water column sufficient enough to weaken the formation of North Atlantic Deep Water (NADW) and northward surface flow in the Atlantic,

thus causing a change in climate via redistributing heat normally transported by the NADW overturning cell. Tracers of deep water production support the hypothesis that changes in NADW formation are coincident with climate change during the Younger Dryas, a 1,300 year long cold event that began about 13 kyr BP (Boyle and Keigwin 1987; Keigwin et al. 1991; Bond et al. 1997), as well as during Heinrich events (Keigwin et al. 1994; Oppo and Lehman 1995; Vidal et al. 1997; Zahn et al. 1997; Curry et al. 1999). While abrupt climate change was once thought to be limited to high latitudes, there is a growing body of evidence suggesting that millennial-scale climate change affects regions around the globe (e.g. Behl and Kennett 1996; Peterson et al. 2000; Wang et al. 2001; Altabet et al. 2002).

Historically, simulations of a Younger Dryas-type event via freshwater forcing in the high-latitude North Atlantic were perceived as contradictory to paleoclimate data for the Younger Dryas because they fail to simulate large changes outside of high-latitude regions despite evidence that the Younger Dryas was a nearly global event (e.g. Cane 1998; Clement et al. 2001). The apparent disagreement between models and the paleodata, as well as the global impact of tropical interannual variability (ENSO; Wallace and Gutzler 1981; Deser and Blackmon 1995; Lau and Nath 1996; Lau 1997; Klein et al. 1999; Schmittner et al. 2000) has led some to suggest that the tropics, rather than the high latitudes, drive millennial-scale climate changes on a global scale (Cane 1998; Clement and Cane 1999; Clement et al. 2001; Yin and Battisti 2001). As the number of freshwater forcing experiments and paleoclimate reconstructions grows, however, it is important to reassess the ability of the models to simulate a Younger Dryas-type cooling.

In this paper, we explore the linkages between North Atlantic climate variability and tropical Atlantic climatology with a three-member ensemble of North Atlantic freshwater forcing experiments using the GFDL R30 coupled Ocean–Atmosphere General Circulation Model (OAGCM).

In particular, we address the following questions:

1. What is the response of the tropical Atlantic region to a cooling of the North Atlantic and a slowdown of meridional overturning circulation?
2. What are the mechanisms driving these responses?
3. How do the results of these experiments compare to paleoclimate data from the Younger Dryas cold event?
4. How sensitive are the results to slight variations in the starting conditions of the experiment?
5. How do the results of these experiments compare to freshwater forcing experiments performed using other models?

We focus on the tropical Atlantic for several reasons. The tropics have been at the center of a debate regarding the mechanisms of millennial-scale climate change (e.g. Cane 1998), yet few North Atlantic fresh-

water forcing studies have specifically examined the tropical response. In addition, there are many recent paleoclimate studies of the Younger Dryas that have focused on the tropical Atlantic region. This, therefore provides a strong basis for the comparison of our model results to paleoclimate data.

## 2 Models and methods

The model used in this study consists of coupled general circulation models of the atmosphere and the ocean, with land surface and sea-ice components also included. This model is identified as GFDL\_R30\_c in the nomenclature of the IPCC TAR [see Table 9.1 of Cubasch et al. (2001)]. The GFDL\_R30\_c model is similar to earlier versions of GFDL coupled models (e.g. Manabe et al. 1991), but with enhanced horizontal and vertical resolution. The description of the model in this section is brief and intended to emphasize the basic characteristics of the model, and the reader should refer to Delworth et al. (2002) for a more complete description.

The atmospheric component employs the spectral transform method with rhomboidal truncation at zonal wave number 30, corresponding to a transform grid spacing of approximately 2.2° latitude by 3.75° longitude. Fourteen unevenly spaced sigma coordinate levels are used for vertical differencing. Insolation at the top of the atmosphere varies seasonally, but not diurnally, and clouds are predicted whenever the relative humidity exceeds a critical threshold. The land-surface model features prognostic snow cover and soil moisture based on a simple “bucket” model. Surface temperature is determined diagnostically, based on the assumption that there is no heat stored in the soil.

The ocean component of the coupled model is based on Version 1.1 of the Modular Ocean Model (Pacanowski et al. 1991), which solves the primitive equations of motion using the Boussinesq, rigid-lid and hydrostatic approximations. The horizontal grid spacing is 2.25° latitude by 1.875° longitude, with depth as the vertical coordinate and 18 unevenly spaced levels. Sea ice is simulated by a simple thermodynamic model, in which ice is treated as a single layer with no sensible heat content. Sea ice is advected by ocean currents, but additional convergence is not permitted once the sea-ice thickness exceeds a critical value (4 m). The formation of leads is not included. The atmospheric and oceanic components of the model exchange fluxes of heat, water and momentum once a day. The heat flux consists of the radiative, sensible and latent components, and the water flux includes evaporation, sublimation, precipitation and runoff from the continents.

As the first step in initializing the fully coupled model, the atmospheric component of the coupled model is integrated using observed seasonal cycles of sea-surface temperature and sea ice as lower boundary conditions, along with a prescribed seasonal cycle of solar radiation at the top of the atmosphere.

In the second step, the ocean component of the coupled model is integrated for several thousand years starting from an isothermal, isohaline state at rest. Climatological monthly mean fluxes of heat, water, and momentum archived from the atmosphere-only integration described above are supplied to the ocean as forcing terms at the sea surface. In addition, sea-surface temperature (SST), sea-surface salinity (SSS), and sea ice are restored to an observed climatological seasonal cycle with a restoring time of 40 days. The model is run until long-term drifts in deep ocean temperature and salinity become relatively small.

Because the two component models are not necessarily in balance with each other, the SSTs computed by the ocean model generally will not match the SSTs to which they are being restored. The restoring terms in the last several hundred years of the ocean component spin-up are averaged to produce spatially and seasonally varying flux adjustment terms, which are added to the atmospheric fluxes passed to the ocean component of the coupled model. The flux adjustments are determined prior to the start of the coupled model integration and do not vary from one year to the next. Because the flux adjustments are independent of the state of the coupled model, they do not systematically damp or amplify anomalies of sea-surface temperature or sea-surface salinity. The use of flux adjustments is successful in greatly limiting the long-term drift of the model (Manabe et al. 1991).

## 2.1 Control run simulations

After coupling the ocean and atmosphere components of the model, a control run (CTRL1) was integrated for

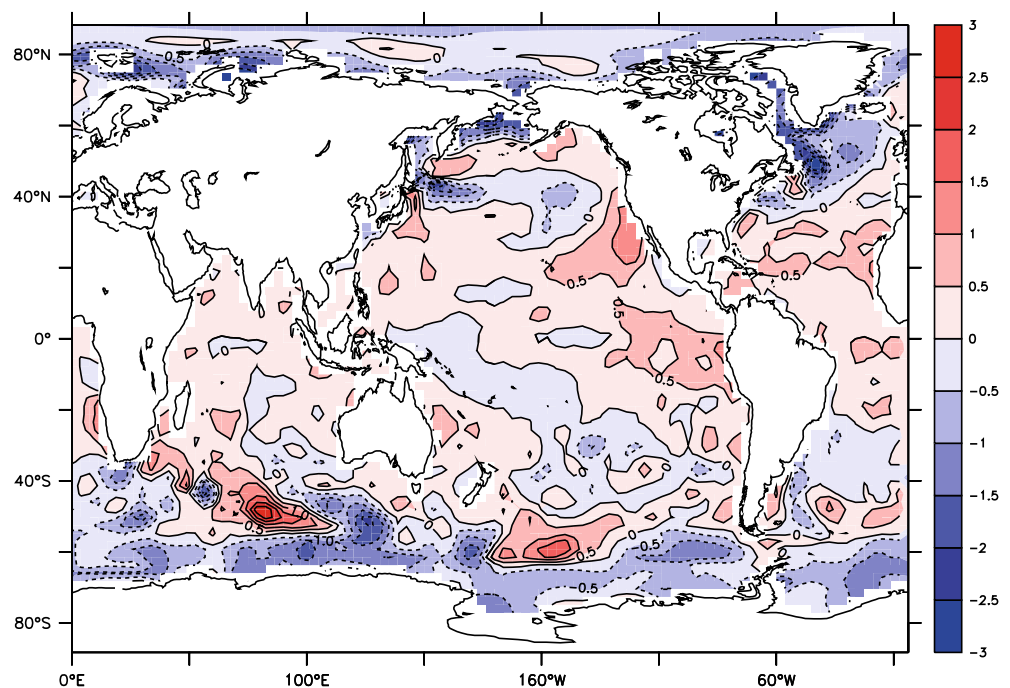
900 years. A second control run (CTRL2) was integrated for 600 years starting from year 601 of CTRL1 and using the same model parameters, but on another computing system. Sea-surface temperatures from the two control runs match within  $0.25^{\circ}\text{C}$  throughout the Atlantic. Within the tropical Atlantic, the difference in SST between the two runs is generally less than  $0.05^{\circ}\text{C}$ . The precipitation patterns exhibited by the two control runs are similar for both December/January/February (hereafter DJF) and June/July/August (hereafter JJA).

The largest differences in SST and precipitation between the two control runs are significantly smaller than the anomalies that result from the freshwater forcing experiments discussed here. We therefore conclude that the differences between the two control simulations are within the range of the internal variability of each run.

Simulated and observed sea-surface temperatures agree well throughout the globe (Fig. 1). In most cases, the difference between observed and simulated temperatures is less than  $1^{\circ}\text{C}$ . Notable exceptions include patches of the Southern Ocean and the region south of Greenland. In these locations, the difference between modeled and observed SSTs is  $2\text{--}3^{\circ}\text{C}$ . The overall pattern of SST in these regions, however, is represented well by the model.

Figure 2 compares the DJF and JJA simulated precipitation with observation data from 1979–2002 (Xie and Arkin 1997). The model is able to simulate the primary features of the observed precipitation patterns. During both DJF and JJA, the model precipitation tends to overestimate precipitation over land, while underestimating precipitation over the oceans. During DJF, the model simulates excess precipitation over portions of South America and southern Africa. During JJA, the modeled precipitation over equatorial Africa is

**Fig. 1** Differences between simulated and observed annual sea-surface temperatures. Simulated temperatures are from years 1 to 900 of CTRL1. Observed data are from Levitus and Boyer (1994)



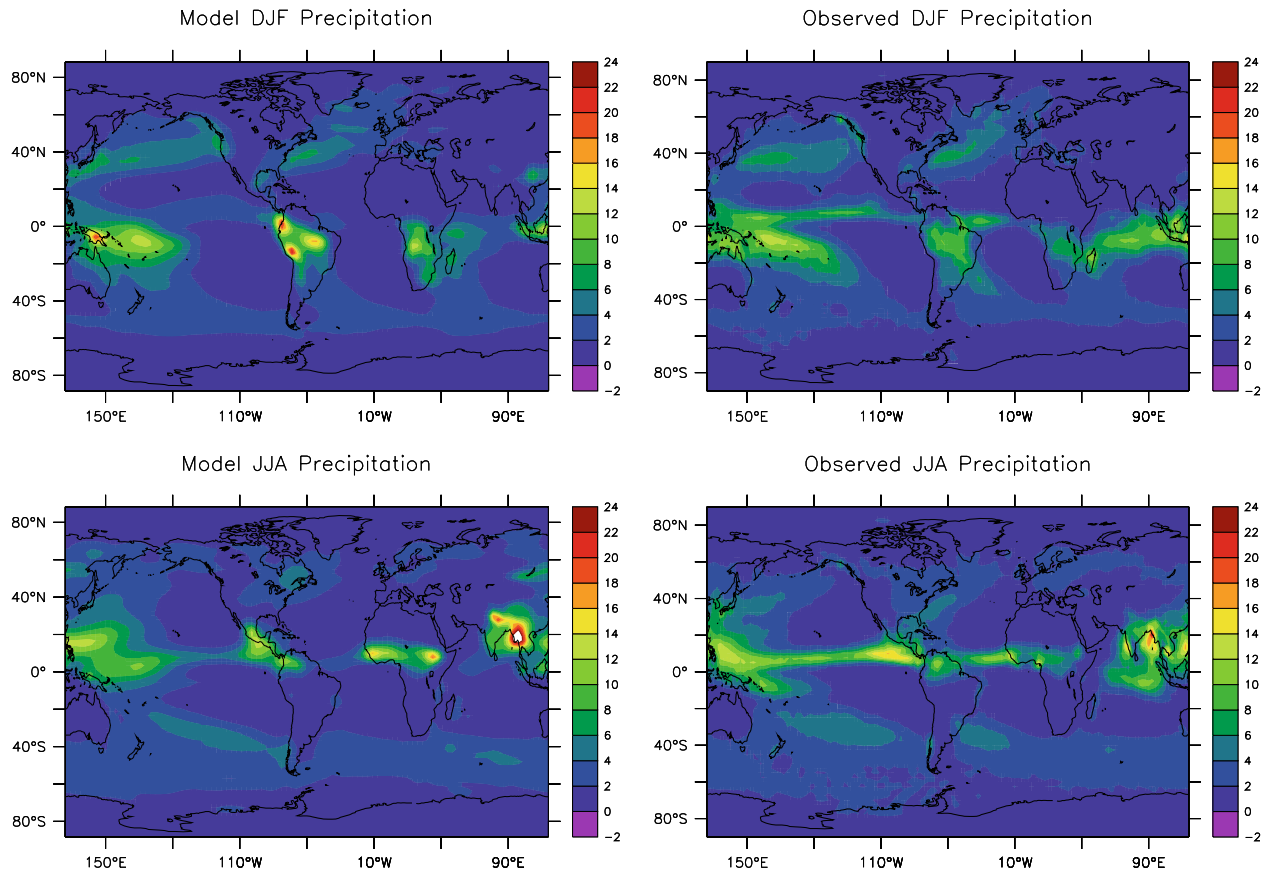


**Fig. 2** Simulated and observed precipitation patterns for DJF (*top*) and JJA (*bottom*). Units are in  $\text{mm day}^{-1}$ . Simulated precipitation is from years 1 to 900 of CTRL1. Observation data are long-term averages from 1979 to 2002 (Xie and Arkin 1997)

too high. These regions of excess precipitation in both seasons correspond to the location of the Intertropical Convergence Zone (ITCZ) in each season. The position of the ITCZ in each season, however, is well captured by the model.

Simulated meridional overturning circulation (MOC) in the North Atlantic varies on multidecadal timescales between 20 Sv and 28 Sv for both CTRL1 and CTRL2. Such variability was observed in lower resolution versions of the GFDL model (Delworth et al. 1993, 1997; Delworth and Mann 2000). The mechanisms driving the variability, however, are not well understood (Delworth et al. 2002). The average value of the MOC (24.6 Sv) is somewhat stronger than current observations of NADW formation in the North Atlantic based on chlorofluorocarbon inventories (17 Sv; Smethie and Fine 2001),

and direct measurements (13 Sv; Dickson and Brown 1994, and references therein).

## 2.2 Freshwater forcing experiments

An ensemble of three freshwater forcing experiments was performed (Table 1). The experiment FW1 was initialized from year 301 of the control run CTRL1. Experiments FW2 and FW3 were initialized from years 601 and 701 of CTRL2, respectively. In each experiment, 0.1 Sv ( $1 \text{ Sv} = 10^6 \text{ m}^3 \text{ s}^{-1}$ ) of freshwater was applied for 100 years across the Atlantic from  $50^\circ\text{N}$  to  $70^\circ\text{N}$ . The freshwater had a temperature equal to that of the ambient SST. At the end of the 100 year period, the freshwater was turned off and the recovery monitored.

**Table 1** List of experiments discussed in this study

Experiment name	Forcing	Length/Description
CTRL1	Control	900 year integration
CTRL2	Control	600 year integration; Initialized from year 601 of CTRL1
FW1	0.1 Sv freshwater	100 years of freshwater forcing; 140 year integration; Initialized from year 301 of CTRL1
FW2	0.1 Sv freshwater	100 years of freshwater forcing; 200 year integration; Initialized from year 601 of CTRL2
FW3	0.1 Sv freshwater	100 years of freshwater forcing; 200 year integration; Initialized from year 701 of CTRL2

Having three experiments with identical freshwater forcing conditions allows us to assess the robustness of relatively small responses.

The surface flux of freshwater applied during these experiments ( $1.6 \times 10^{-6} \text{ cm s}^{-1}$ ) is three orders of magnitude greater than the surface salinity flux adjustment within the same box in North Atlantic ( $3.4 \times 10^{-9} \text{ cm s}^{-1}$ ). The flux adjustments, which do not vary temporally or between experiments, are such that freshwater is being removed from the North Atlantic region. Because they do not vary temporally or between experiments, the flux adjustments should not systematically damp or amplify the response to freshwater forcing.

The rate of 0.1 Sv is comparable to estimates of glacial meltwater (Licciardi et al. 1999) and ice-rafted debris (MacAyeal 1993) inputs into the North Atlantic during the Younger Dryas. The duration of the freshwater pulse in these experiments is shorter than that inferred for meltwater pulse 1 A (MWP1A), which is inferred to have been associated with the Younger Dryas (Fairbanks 1989); therefore, the total freshwater input during the experiment is less than implicated for MWP1A. The discharge location of MWP1A, and its relationship to the Younger Dryas is unclear (e.g. Fairbanks 1990; Weaver et al. 2003). While we compare our results to paleoclimate data from the Younger Dryas, it should be noted that the experiments discussed here were run from modern-day boundary conditions rather than glacial or Bølling/Allerød boundary conditions. Most significantly there are no ice sheets over North America and Eurasia in our control runs, and insolation is set at modern-day levels.

Unless stated otherwise, all anomalies shown are the ensemble mean anomalies of the three FW experiments. Anomalies for FW1 were calculated using the last 25 years of the experiment run and CTRL1 while anomalies for FW2 and FW3 were calculated using the last 20 years of each experiment run and CTRL2. In each case, the time mean average of the entire available control run (i.e. 900 years for CTRL1 and 600 years for CTRL2) was used. The three individual anomalies were then averaged in order to determine the ensemble mean anomaly.

### 3 Results and discussion

#### 3.1 Model results

##### 3.1.1 Atlantic results

In each freshwater forcing experiment, North Atlantic MOC decreases by  $\sim 10$  Sv by the end of the freshwater pulse (Fig. 3). MOC decreases rapidly at the onset of each freshwater forcing. The decrease continues at a slower rate throughout the remainder of the experiments, and is punctuated by a series of decadal-scale oscillations in the strength of MOC. The decrease in

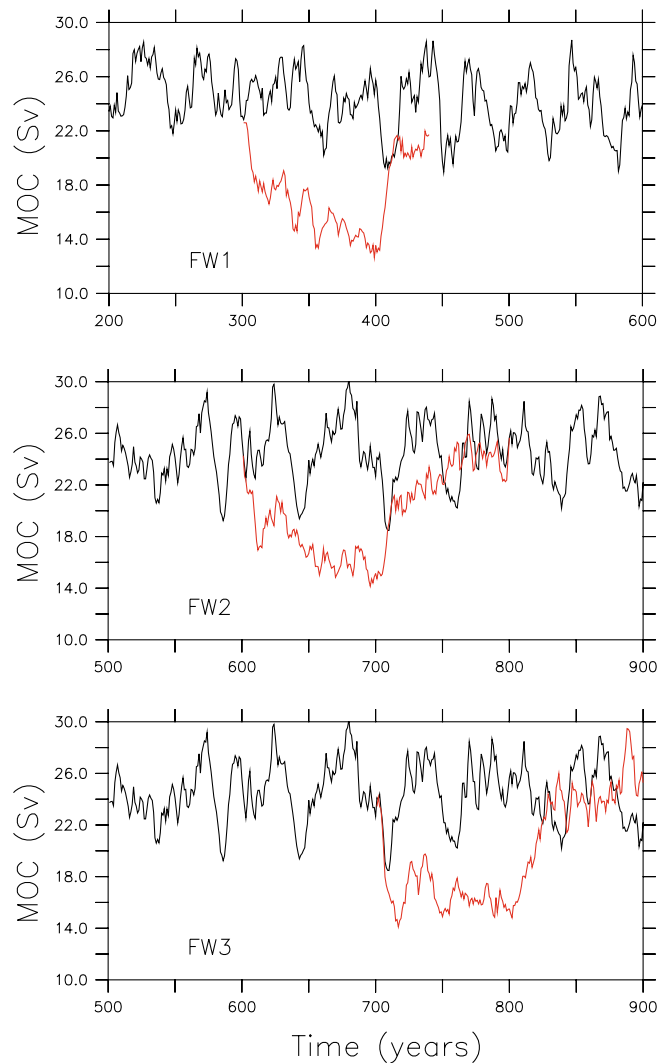


**Fig. 3** Time series of North Atlantic meridional overturning circulation during the control runs (black) and experiments (red) for FW1 (top), FW2 (middle) and FW3 (bottom)

MOC is caused by the development of a low-salinity cap over the North Atlantic that prevents sinking and formation of deep waters (Fig. 4, top). Salinity in the North Atlantic is up to 3 psu lower during the experiments than during the control runs. Formation of Antarctic Bottom Water (AABW) increases and penetrates as far north as  $40^\circ\text{N}$  during the freshwater experiments. These results are generally consistent with those of other modeling studies that show a slowdown of North Atlantic Deep Water (NADW) and enhanced AABW formation in response to a North Atlantic freshwater input (Manabe and Stouffer 1995; Rahmstorf 1995; Manabe and Stouffer 1997; Schiller et al. 1997). North Atlantic MOC in each FW experiment recovers to near its initial values within 50 years of the termination of the freshwater pulse.

As a result of the decrease in MOC, North Atlantic SSTs decrease by up to  $11^\circ\text{C}$  (Fig. 4, middle). There is a slight cool bias in the control run (Fig. 1) where the

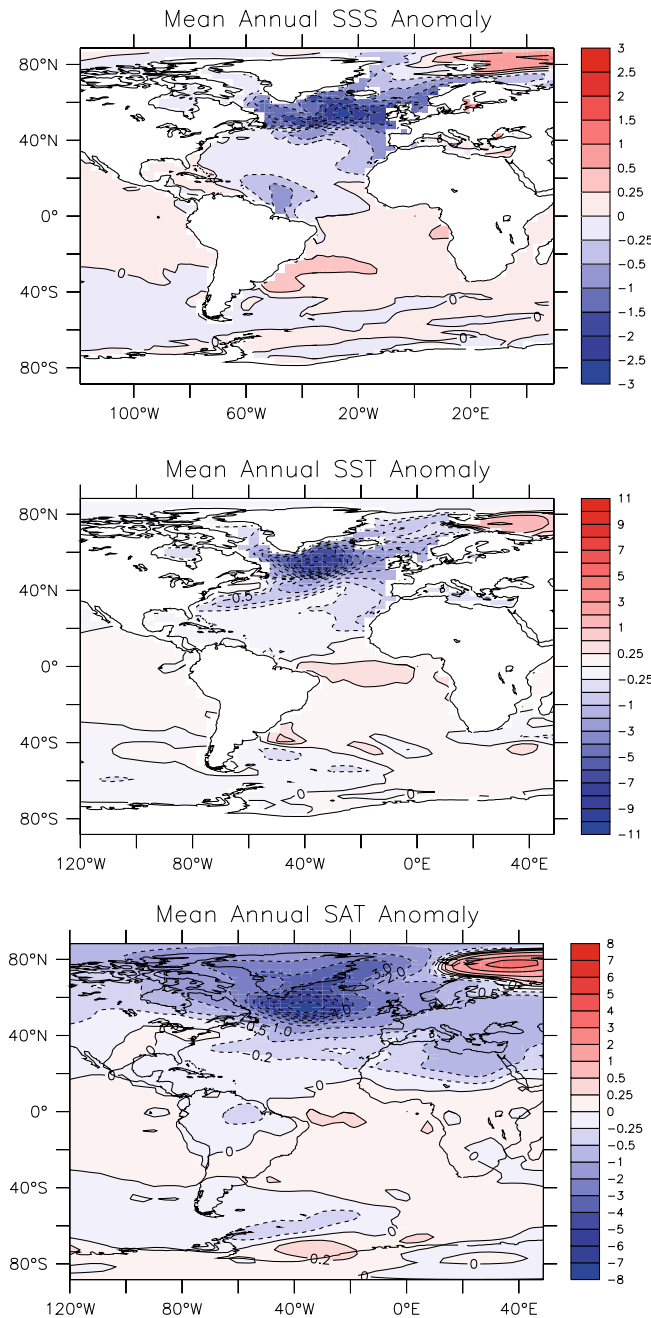


**Fig. 4** Ensemble mean anomalies averaged over the last 20–25 years of each experiment. Anomalies are expressed as experiment minus control. *Top* sea-surface salinity anomaly, units are parts per thousand (ppt). *Middle* sea-surface temperature anomaly. *Bottom* surface-air temperature anomaly

greatest cooling occurs in the FW experiments that may contribute 1°C to the cool anomalies. While centered in the northern North Atlantic, the cool anomalies extend as far south as 10°N in the Atlantic. Outside of the Atlantic basin, there are no statistically significant SST anomalies. Surface-air temperatures (SATs) exhibit a similar response (Fig. 4, bottom). In the northern North Atlantic, SAT decreases by up to 8°C. This anomaly is centered just south of Greenland. The cooling extends

through northern Africa. Interestingly, both the SST and SAT of the Barents Sea region warm during the freshwater forcing experiments as a result of decreased sea ice in the Barents region. The Barents Sea warming and sea ice reduction could be sensitive to the location in which the freshwater is applied, as the warming occurs north of the region into which freshwater was introduced. The pattern of sea ice anomalies produced by the freshwater forcing, namely increased sea ice south of Greenland and decreased sea ice in the Barents Sea, is reminiscent of the 9–10 year sea ice oscillations, noted by Venegas and Mysak (2000), based on century-long North Atlantic sea-ice records. The model response shows an increase in the strength of the Norwegian Current, which Venegas and Mysak (2000) identify as a likely mechanism for decreasing sea-ice concentrations in the Barents Sea.

### 3.1.2 Tropical Atlantic results

The cooling of the North Atlantic decreases in magnitude from high to low latitudes. The gradient of SST anomalies, with cooling to the north and warming to the south, is steep in the western tropical Atlantic and more gradual in the eastern tropical Atlantic. SSTs throughout the tropical Atlantic (5°N–20°S, 40°W–20°E) warm by 0.2°C (Fig. 5, top), with anomalies greater up to 0.4°C in the western tropical Atlantic. The magnitude of the interannual variability in tropical Atlantic SST is in the order of the anomalies exhibited during the FW experiments. However, a two-tailed *t*-test demonstrates that all of the anomalies discussed in the manuscript are significant at the 95% confidence level. The temperature anomaly increases with depth and has a maximum of 4.5°C in the thermocline off the coast of South America (Fig. 6). The warm thermocline anomaly begins to develop at the onset of the freshwater forcing and increases steadily throughout the experiment. Tropical Atlantic SSTs, however, cool for the first 20 years of the experiment before gradually warming. The SST response may be damped with respect to that of the thermocline due to air–sea processes. The warm anomalies most likely result from a decrease in the surface and thermocline return flow of warm waters from the tropics to the North Atlantic. Because the formation of deep water in the North Atlantic decreases during the freshwater forcing experiments, less water must flow northward in order to compensate for the export of deep water from the Atlantic. At the surface, northward velocity in the North Brazil Current decreases by 15–25%. In the thermocline, northward velocities, normally 1–3 cm s<sup>-1</sup> in the control runs, decrease by up to 50%.

Regressing SST against North Atlantic MOC in the control runs allows us to observe the natural, unforced relationship between SST and MOC in the model. This relationship can then be compared to the anomalies generated during the FW runs. For a 1 Sv increase in MOC in the control runs, tropical Atlantic SSTs cool by up to 0.02°C (Fig. 7). Assuming that this cooling is due

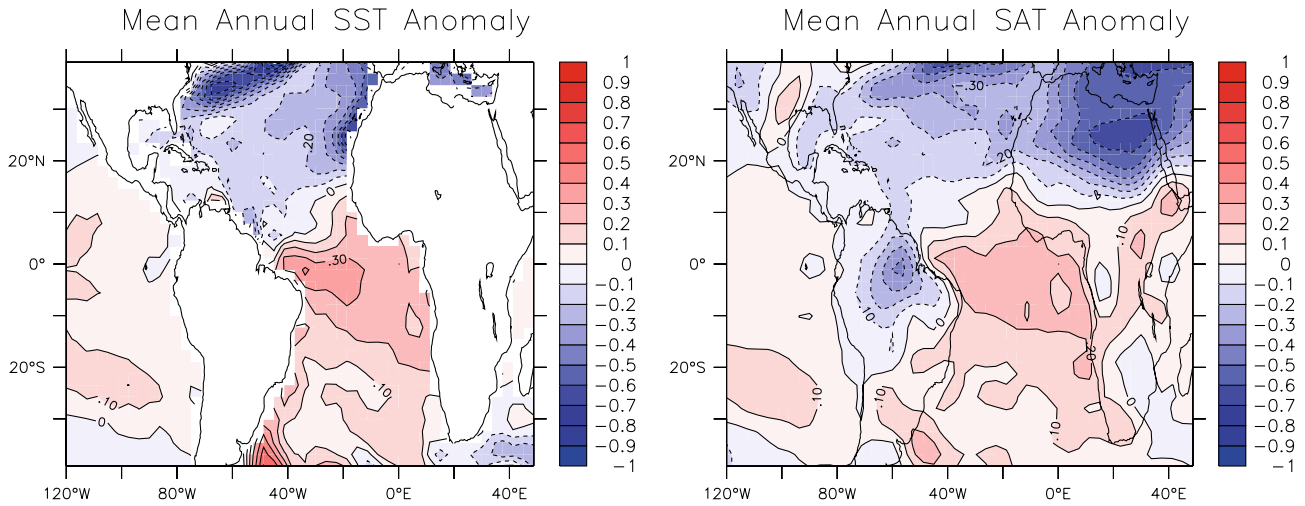


**Fig. 5** Ensemble mean tropical Atlantic SST (*left*) and SAT (*right*) anomalies averaged over the last 20–25 years of each experiment Units are °C

entirely to the increase in MOC and that the relationship is linear, a 10 Sv decrease in MOC would result in a 0.1–0.2°C warming of tropical Atlantic SST. The SST anomalies that result from the freshwater forcing are therefore consistent with the relationship between tropical Atlantic SST and MOC in the control run.

Surface-air temperatures in the tropical Atlantic cool north of 10°N. The magnitude of the cooling decreases progressively southward (Fig. 5, bottom). South of 10°N, SAT decreases by up to 0.1–0.5°C over northern South America, but increases by 0.2°C over the ocean and the southern half of Africa. The dichotomy of cooling over South America and warming over Africa is the result of the precipitation changes over the two continents. As will be discussed subsequently, precipi-

tation, and consequently soil moisture, over northern South America generally increases during the freshwater forcing experiments. As a result of the increased soil moisture, an increased proportion of incoming radiation must be devoted to evaporation of the moisture (i.e. latent heating) as opposed to heating the air (i.e. sensible heating). The net effect is, therefore, a cooling of SAT over South America. The opposite is true for Africa; i.e. the general drying of Africa allows for a decrease in latent heating and, therefore, a warming of SAT over the continent. The SAT warming over the ocean is consistent with the warming of SSTs discussed above.

During the FW experiments, the Northeast trade winds become stronger in both winter and summer while the Southeast trade winds experience little or no change

**Fig. 6** Cross-sectional view (averaged from 5N to 20S) showing the ensemble mean temperature anomaly in the tropical Atlantic thermocline. Anomalies represent the ensemble mean of the three hosing experiments, averaged over the last 20–25 years of each experiment. Units are °C

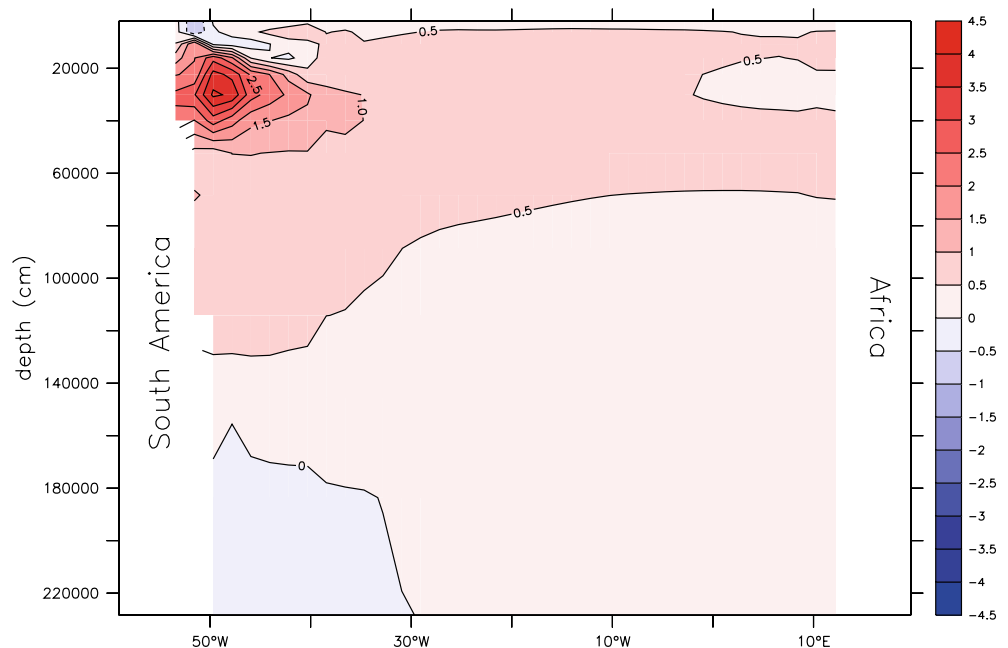


**Fig. 7** Regression of SST onto North Atlantic meridional overturning circulation for years 1–900 of the control run (CTRL1). These are the SST anomalies that result from a 1 Sv increase in MOC. Units are  $^{\circ}\text{C}$

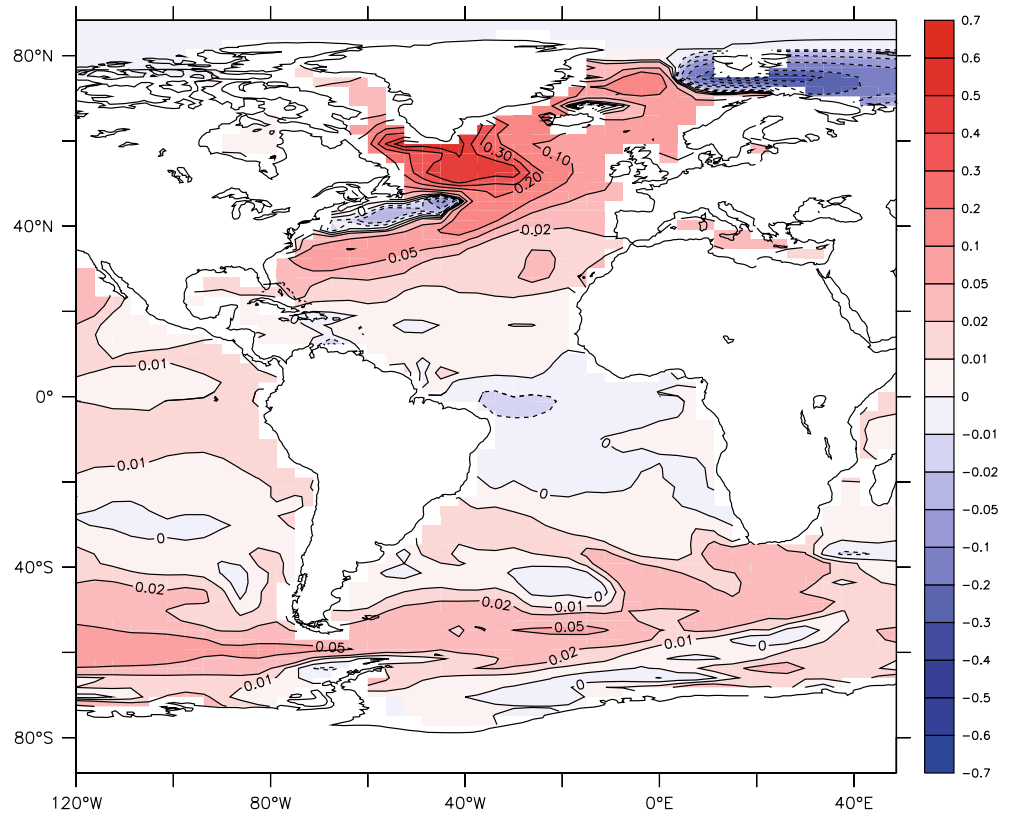
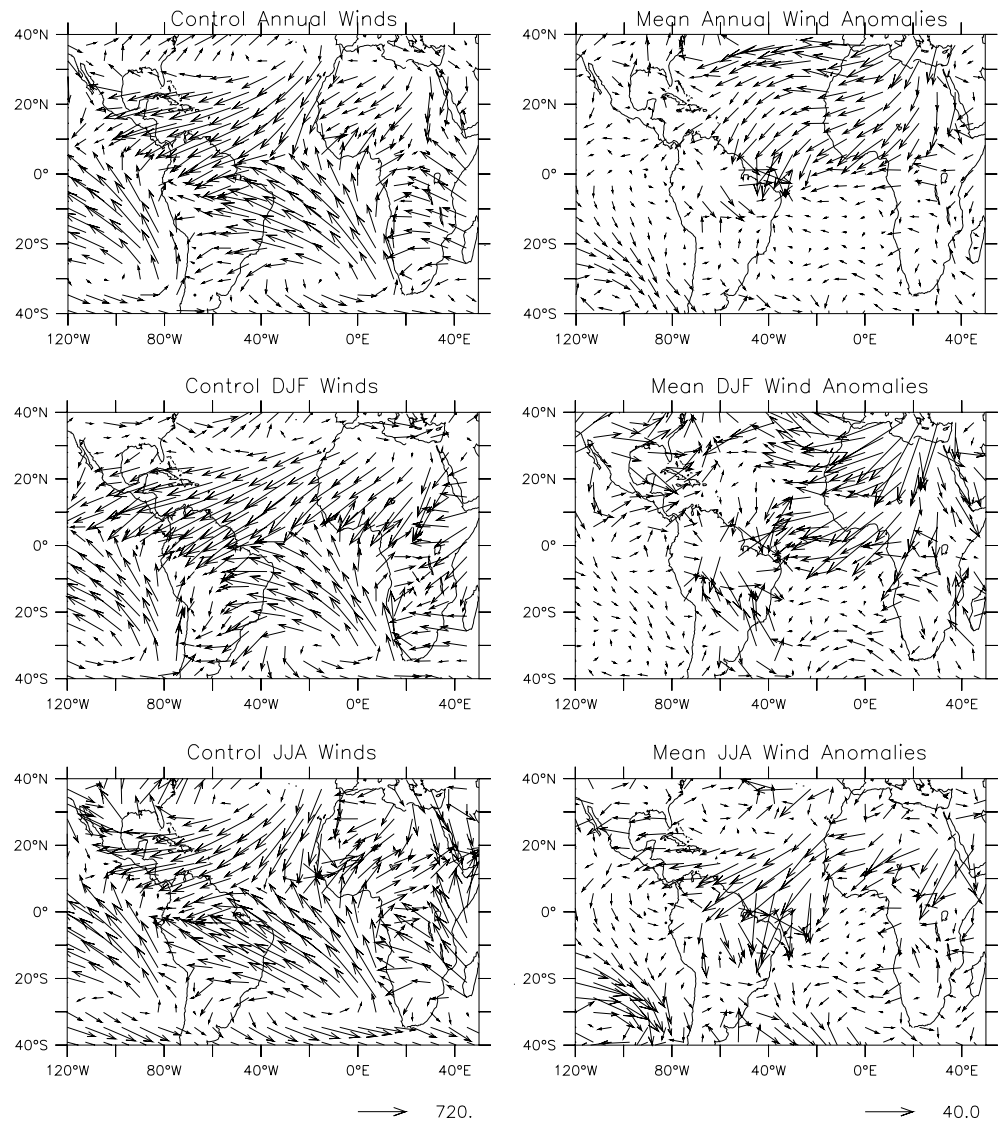


(Fig. 8). Upwelling within the upper 100 m of the water column increases in the northern tropics ( $5\text{--}10^{\circ}\text{N}$ ) and decreases in the southern tropics ( $0\text{--}10^{\circ}\text{S}$ ). These upwelling changes may help to reinforce the SST anomalies observable in Fig. 5. In association with the changes in trade wind strength, the mean position of the Intertropical Convergence Zone (ITCZ) shifts southward. In nature, the position of the ITCZ is one of the dominant controls on precipitation patterns in the Atlantic region (as well as the rest of the tropics). During the Northern Hemisphere summer, the ITCZ is at its northernmost position, residing around  $10^{\circ}\text{N}$ . During this time, there is relatively high precipitation in Central America and across the Sahel region of Africa. The ITCZ then migrates southward during Northern Hemisphere winter. Because this southward migration causes the ITCZ to fall over the continent of South America, the ITCZ becomes less latitudinally defined (Waliser and Gautier 1993). Zones within northern South America experience high precipitation during this time. In Africa, the southward migration of the ITCZ and Zaire Air Boundary (ZAB; the boundary between winds from the Atlantic and the Indian Oceans) leads to high precipitation in the southern half of the continent (Nicholson 2000).

The precipitation anomalies associated with the freshwater forcing experiments are consistent with a southward shift in the mean position of the ITCZ (Fig. 9). JJA precipitation anomalies show a decrease in the Sahel region of Africa and an increase in precipita-

tion over coastal equatorial Africa and Northeast Brazil (NEB). These anomalies occur in a latitudinally oriented configuration, which suggests that they are driven by changes in the position of the ITCZ. The freshwater forcing induces a strong increase in precipitation in NEB during both DJF and JJA. The DJF increase is stronger than the JJA increase, likely due to increased advection of moisture from the Atlantic ocean by the strengthened NE trades. As shown in Fig. 8, the DJF wind anomalies are strongest over the equatorial Atlantic, while the JJA anomalies are strongest over the tropical–subtropical Atlantic. The strengthened DJF winds are thus gaining moisture from regions of the ocean that show a SST warming anomaly during the FW experiments. In contrast, JJA winds are blowing over higher latitude oceanic regions that undergo a cooling during the FW experiments, therefore decreasing moisture availability over the ocean. The increase in South American precipitation during DJF is associated with an increase in both high and low cloud cover (not shown) over northeast Brazil that results from the convergence of winds over northern South America (Fig. 8). In contrast, precipitation in equatorial–subequatorial Africa generally decreases during Northern Hemisphere winter. This drying may be induced by a change in the strength and direction of the winds contributing to the ZAB. During the freshwater forcing experiments, onshore winds from the Atlantic decrease slightly (5%) in strength while onshore winds from the Indian Ocean become more northerly in direction. Thus, during the freshwater forcing experi-

**Fig. 8** Control (left) and anomalous (right) winds for ANN (top), DJF (middle), and JJA (bottom). Anomalies represent the ensemble mean of the three hosing experiments, averaged over the last 20–25 years of each experiment. Note the vectors for scale. Units are  $\text{cm s}^{-1}$



ments, the convergence of the two wind systems, which is a source of DJF precipitation in the southern half of Africa, decreases. As a result, DJF rainfall decreases in this region of Africa.

The response to the southward shift of the ITCZ in the Atlantic sector is similar to the response noted by Chiang et al. (2003, hereafter CBB) in a simulation of the Last Glacial Maximum, in which insolation,  $\text{CO}_2$ , and land ice were set to their presumed 21 kyr values. They attribute the responses they observe to a “meridional mode” of atmosphere–ocean variability associated with a strengthening of the Northeast trade winds. The response of the ITCZ in the FW experiment is also accompanied by the changes in trade wind strength and the meridional SST gradient, as in CBB. To quantify this similarity, we used the anomalies of the FW experiment with respect to the control to compute the same indices of North tropical Atlantic trade wind strength and meridional SST gradient defined by CBB. The signs of these two indices in the FW experiments are consistent with CBB’s LGM simulation,

although the magnitudes are smaller, which suggests that a similar physical mechanism may be operative.

Some insight into the physical mechanism responsible for the southward shift of the ITCZ in the Atlantic sector in the freshwater forcing simulations can be taken from the experiments of Broccoli et al. (in preparation), who examined the response of tropical climate to extratropical thermal forcing using an atmosphere–mixed layer ocean model. The atmospheric component of this model was virtually identical to the atmospheric component of the current coupled model, but the oceanic component consisted of an isothermal, static slab of water of 50 m depth. Instead of realistic geography, two flat continents, symmetric about the equator, were used to simplify the interaction between continental configuration and climate. This simulation is hereafter identified as the SYMM integration. A second integration was also made, in which an additional heat flux of  $-10 \text{ W m}^{-2}$  was applied to the slab ocean north of  $40^\circ\text{N}$  and a positive flux of the same magnitude was applied

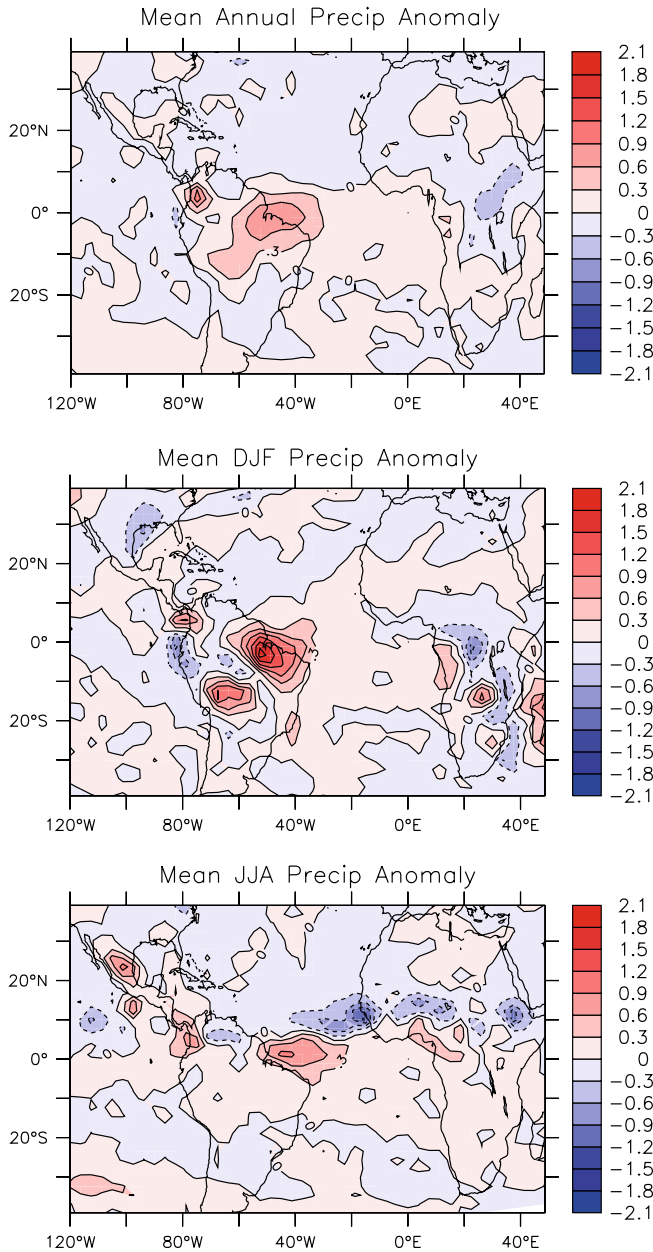


**Fig. 9** Ensemble mean precipitation anomalies for ANN (*top*), DJF (*middle*), and JJA (*bottom*). The anomalies represent the last 20–25 years of each experiment. Units are  $\text{mm day}^{-1}$

south of  $40^{\circ}\text{S}$ . This Cool North Warm South (hereafter CNWS) integration can be regarded as analogous to the FW experiments, in which a large surface cooling takes place in the extratropical North Atlantic with little systematic change in surface temperature elsewhere. For comparison, the zonally averaged heat flux anomaly north (south) of  $40^{\circ}\text{N}$  ( $40^{\circ}\text{S}$ ) for the cooling associated with the FW experiments is  $4 \text{ W m}^{-2}$  ( $0.4 \text{ W m}^{-2}$ ) and is centered in the North Atlantic with little change elsewhere. The anomalous heat fluxes prescribed for CNWS are therefore much larger than the heat flux anomalies generated during the FW experiments. In response to the extratropical thermal forcing, the ITCZ in the CNWS

integration shifts southward, antisymmetric precipitation anomalies straddle the equator, and the northern trade winds are enhanced while the southern trades are weakened (Fig. 10). Each of these features is qualitatively similar to those appearing in the FW experiments in the Atlantic sector, albeit in a more exaggerated form. If one assumes that the similarity of the FW and CNWS responses is indicative of a similarity in mechanism, then the following chain of causation, described in more detail for the CNWS case by Broccoli et al. (in preparation), is responsible for the tropical Atlantic response in the FW experiments. The North Atlantic cooling that results from the weakening of the MOC strengthens the pole-to-equator temperature gradient in the Atlantic sector, causing the northern extratropics to demand more heat from the tropics. The atmospheric mean meridional circulation satisfies this increased demand by shifting southward in order to transport heat from the equator to high latitudes. The changes in ITCZ position, tropical precipitation, and trade wind strength are thus a response to a change in the mean meridional circulation of the atmosphere in the Atlantic sector.

In addition to the position of the ITCZ, tropical Atlantic SST patterns provide controls on precipitation in South America and Africa. Many studies have suggested that there is a positive correlation between rainfall in NEB and tropical Atlantic SST anomalies (Markham and McLain 1977; Hastenrath and Heller 1977; Mechoso et al. 1990) and/or the meridional SST gradient in the tropical Atlantic (Moura and Shukla 1981; Uvo et al. 1998). The extent to which tropical Atlantic SSTs influence rainfall in NEB varies on both seasonal (e.g. Uvo et al. 1998) and interannual (e.g. Folland et al. 2001; Peagle and Mo 2002) timescales. Using the CTRL1 control run, we have regressed precipitation against tropical Atlantic SST averaged from  $5^{\circ}\text{N}$ – $5^{\circ}\text{S}$  across the Atlantic. An increase in tropical Atlantic SST is associated with an increase in precipitation over NEB. This relationship is particularly evident in the regressions of annually averaged precipitation onto annual SST (Fig. 11) and of DJF precipitation onto DJF SST (not shown), which is generally consistent with the findings of Uvo et al. (1998) and Peagle and Mo (2002). It is important to note that in nature, rainfall in South America is also influenced by tropical Pacific SST (e.g. Uvo et al. 1998; Pezzi and Cavalcanti 2001). Given that SST in the tropical Pacific is unchanged in response to the freshwater forcing experiments, however, it is unlikely that SST variability in the tropical Pacific is responsible for the precipitation anomalies that develop in South America. During the freshwater forcing experiment, the increase in tropical Atlantic SST may be contributing to the changes in precipitation over South America. As shown in Fig. 11, a  $1^{\circ}\text{C}$  increase in annually averaged tropical Atlantic SSTs is associated with a  $0.9 \text{ mm day}^{-1}$  increase in annually averaged NEB precipitation ( $30^{\circ}\text{W}$ – $50^{\circ}\text{W}$ ,  $0^{\circ}\text{S}$ – $15^{\circ}\text{S}$ ). Thus the  $0.3^{\circ}$  warming of tropical Atlantic SSTs during the experiments could elevate annual pre-

**Fig. 10** Differences in annually averaged precipitation rate (colors, in  $\text{mm day}^{-1}$  and surface winds (vectors, in  $\text{cm s}^{-1}$  between the CNWS and SYMM integrations

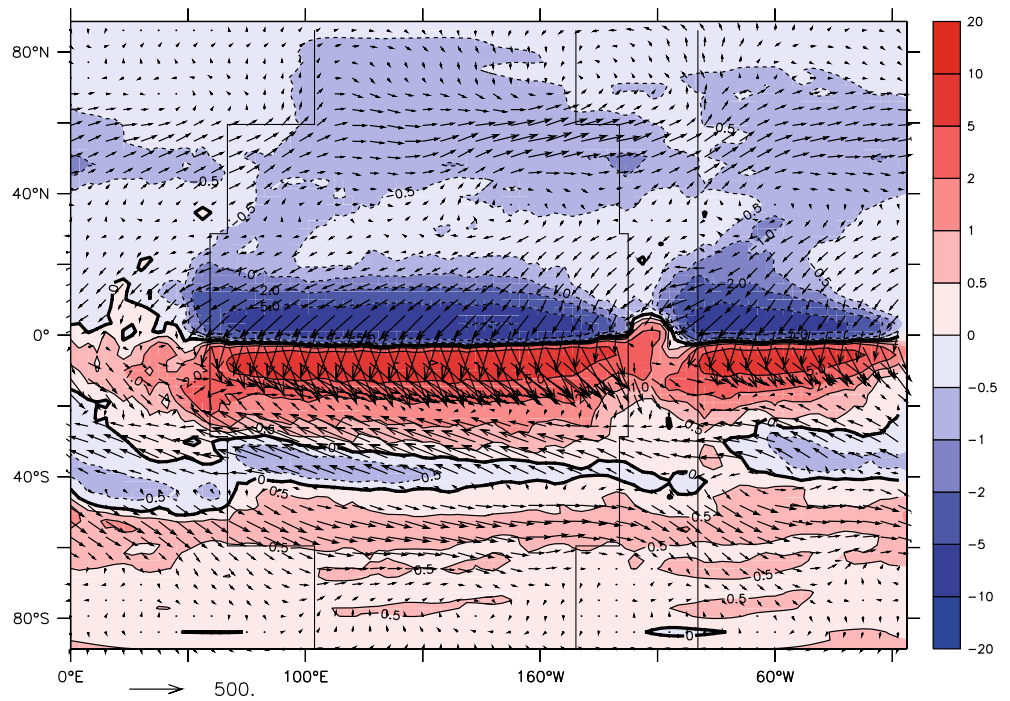
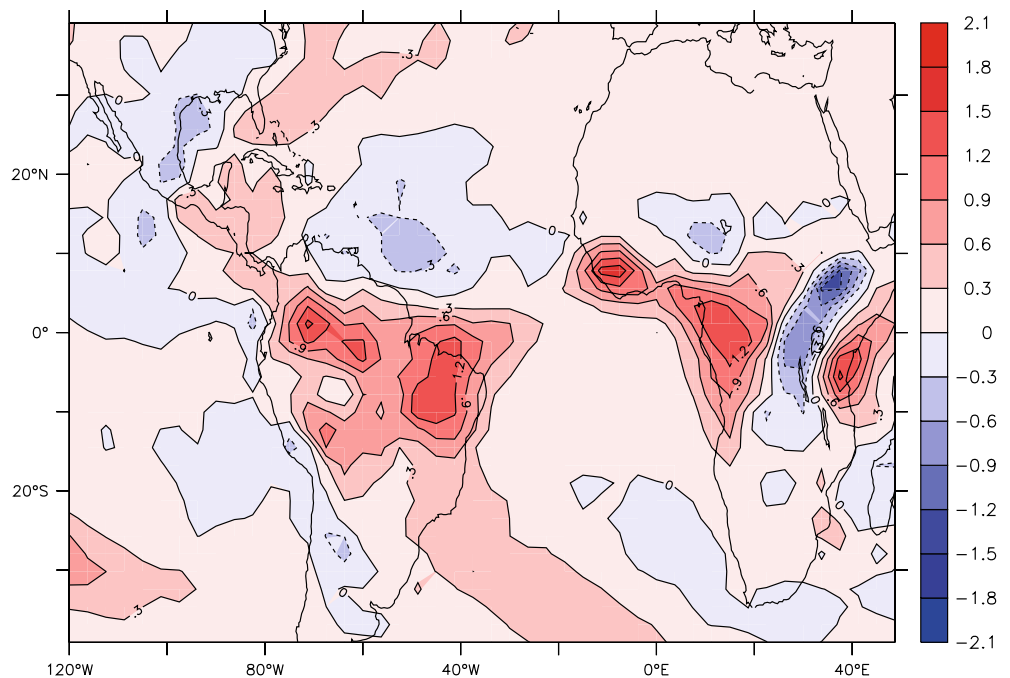


**Fig. 11** Regression of annual CTRL1 precipitation against annual tropical Atlantic SST (averaged 5N–5S, 40W–0E). Units for precipitation are  $\text{mm day}^{-1}$ . The field was scaled such that the figure can be interpreted as a linear response to a  $1^\circ\text{C}$  increase in tropical SST



precipitation in NEB by  $\sim 0.3 \text{ mm day}^{-1}$ , a change that is generally consistent with the results shown in Fig. 9.

Tropical Atlantic SSTs also affect precipitation patterns in Africa. Warm SSTs along the Benguela coast are associated with high coastal rainfall (Nicholson 2000). This can be seen in the control run regression of tropical Atlantic SST and precipitation. On an annual basis, a  $1^\circ\text{C}$  increase in tropical Atlantic SST is associated with a  $1\text{--}2 \text{ mm day}^{-1}$  increase in rainfall along the western coast of Africa (Fig. 11). The slight increase (up to  $0.3 \text{ mm day}^{-1}$ ) in African coastal

precipitation in response to the freshwater forcing (Fig. 9) is consistent with the  $0.3^\circ\text{C}$  increase in tropical Atlantic SST.

Thus, the rainfall anomalies in South America and Africa during the freshwater forcing experiments result from a combination of a southward shift in the ITCZ and an increase in tropical Atlantic SSTs. As mentioned above, the increase in tropical Atlantic SST is most likely a result of the decreased surface return flow that occurs in response to the slowdown of NADW export from the Atlantic.

## 3.2 Comparisons

### 3.2.1 Paleodata-model comparison

A growing number of studies indicate that climate variability on millennial-timescales is not limited to the North Atlantic region. Until recently, such variability was thought to be driven by rapid climate changes in the North Atlantic region, possibly caused by rapid surging of ice sheets and freshwater capping of the North Atlantic. As evidence for millennial-scale climate variability mounts from throughout the globe, however, this paradigm is being reevaluated. In essence, it is unclear whether North Atlantic climate changes can be effectively propagated throughout the globe in order to induce seemingly simultaneous climate change in remote areas (e.g. Cane 1998). Freshwater forcing experiments provide a means for testing the ability of North Atlantic-driven climate change to affect regions outside of the North Atlantic (e.g. Dong and Sutton 2002). Again, however, it must be noted that the boundary conditions for events such as the Younger Dryas were likely to have been very different from the modern day boundary conditions used in these experiments. Nevertheless, the FW experiments have a significant effect on the tropics and it is important to assess which model responses are consistent with paleoclimate data. In each of the studies discussed below, we compare the difference between Bølling/Allerød (the period preceding the Younger Dryas) and Younger Dryas climates as opposed to the difference between Holocene and Younger Dryas climate. The comparison was done in this way in hopes that a Bølling/Allerød to Younger Dryas comparison would be more analogous to the simulation of cooling from modern-day boundary conditions in the freshwater forcing experiments. The tropical Atlantic data discussed in this section are summarized in Table 2, Fig. 12, and 13.

The history of deepwater formation in the Atlantic was reconstructed using the carbon isotopic composition ( $\delta^{13}\text{C}$ ) and Cd/Ca ratio of benthic foraminifera. Both of these proxies are sensitive to the nutrient concentration of the ambient water, which, in theory, varies with the amount of NADW versus AABW at a given site. Several North Atlantic studies of these, and other nutrient-based tracers suggest that there was a decrease in the strength, but not a shutdown, of NADW formation (Boyle and Keigwin 1987; Keigwin et al. 1991; Bond et al. 1997; Marchitto et al. 1998) during the Younger Dryas. Given that these are water-mass tracers rather than kinematic tracers, it is difficult to quantify the reduction in deepwater formation during the Younger Dryas. The direction of the changes documented by these proxies is consistent with the results obtained here.

Paleotemperature reconstructions from the North Atlantic (north of 20°N) suggest that SSTs and SATs cooled during the Younger Dryas. Although the magnitude of this cooling is location-dependent, estimates of the SST and SAT changes in the northern North

Atlantic are on the order of 6–10°C (Dansgaard et al. 1989; Chappellaz et al. 1993; Kroon et al. 1997). Pollen evidence from throughout Europe also suggests a Younger Dryas cooling (e.g. Walker et al. 1994; Ammann et al. 1994; deBeaulieu et al. 1994, and references therein). For a more comprehensive map of North Atlantic sites showing a Younger Dryas cooling, refer to Broecker (1995). The limited paleoclimate data from the Barents Sea suggests that this sea was at least seasonally ice-free during the Younger Dryas (Rosell-Mele and Koc 1997). However, we know of no conclusive studies suggesting temperature changes in the Barents Sea region that would either substantiate or refute the warming response during the FW experiments.

Alkenone-derived SSTs from a well-dated core on the Iberian margin show a 3–4°C cooling during the Younger Dryas and Heinrich Event 1 (H1 Bard et al. 2000). Further south, two alkenone records from the western African margin, as well as a coral record from Barbados, show 1–2°C cooling during the Younger Dryas (Zhao et al. 1995; Guilderson et al. 2001; Kim et al. 2002). A Mg/Ca SST reconstruction from the Cariaco Basin shows a 2–3°C cooling during the Younger Dryas (Lea et al. 2003). Several studies, however, document a warming of tropical Atlantic SSTs during the Younger Dryas. These studies include sites off the coast of Grenada (~1°C, Rühlemann et al. 1999; Lea et al. 2003) along the western African Margin (Mulitza and Rühlemann 2000) and off the coast of NEB (Fig. 12, Arz et al. 1999).

Within the region that experiences warming during the FW experiments, three of the five temperature-reconstruction sites demonstrate a warming during the Younger Dryas. These sites show greater Younger Dryas warming than that generated during the FW experiments. The two sites that experience a cooling are located within upwelling regions, which may not be well simulated by our model.

Surface-air temperature reconstructions from Central and South America generally suggest that these regions cooled during the Younger Dryas (Fig. 13). Pollen-based temperature reconstructions from Costa Rica and Colombia suggest a cooling of 1–6°C. A tropical ice-core record from Huascarán, Peru, also suggests a cooling during the Younger Dryas (Thompson et al. 1995). While the FW experiments do show a cooling of SAT over northern South America, the magnitude of the cooling (less than 0.5°C is smaller than that implied by the paleoclimate data. Furthermore, the cooling of northern South America during the FW experiments is likely due to increased precipitation in the region, which may not be consistent with paleoclimate data from the Younger Dryas.

Reconstructions of aridity from the Americas suggest a pattern of reduced precipitation in northern South America, Central America, and the Caribbean and increased precipitation in southern South America (Fig. 13). Pollen data from Lake Chalco, Mexico (Flores-Diaz 1986), Haiti (Hodell et al. 1991), and Colombia

**Table 2** Summary of Paleoclimate data-model comparisons

Ref#	Location	YD conditions (Type of Data)	Model results	Reference
Atlantic SST data				
1	Iberian Margin	−3–4°C (alkenone SST)	−0–2°C	Bard et al. (2000)
2	North Atlantic (37°N)	−2°C (alkenone SST)	−0.1–0.2°C	Calvo et al. (2001)
3	Northwest African Margin	−1.5°C (alkenone SST)	−0.2–+0.2°C	Zhao et al. (1995)
4	Namibian Margin	−2°C (alkenone SST)	+0.2–0.3°C	Kim et al. (2002)
5	Congo Fan	+1.5°C (alkenone SST)	+0.2–0.3°C	Mulitza and Rühlemann (2000)
6	Southwest African Coast	−1–2°C (mollusc mineralogy and $\delta^{18}\text{O}$ )	+0–0.1°C	Cohen et al. (1992)
7	Barbados	−1–2°C (coral $\delta^{18}\text{O}$ )	−0–0.2°C	Guilderson et al. 2001
8	Tobago Basin	+2°C (foraminifera transfer functions)	+0–0.2°C	Hüls and Zahn (2000)
9	Grenada	+1.2°C (alkenone SST)	−0–0.2°C	Ruhlemann et al. (1999)
10	Northeast Brazil Slope	+1–3°C (planktonic $\delta^{18}\text{O}$ )	+0.1–0.3°C	Arz et al. (1999)
11	Cariaco Basin	−3°C (foraminifera Mg/Ca)	+0–0.2°C	Lea et al. (2003)
12	Gulf of Mexico	cooler (faunal assemblages, $\delta^{18}\text{O}$ )	−0–0.2°C?	Flower and Kennett (1990)
S. American Precip, Wind, and SAT Data				
13	Ceara Rise	NE Brazil dry (Ti/Ca, Fe/Ca)	NE Brazil wet	Arz et al. (1998)
14	Amazon Fan	Amazon Basin dry (planktonic $\delta^{18}\text{O}$ )	Amazon wet	Maslin and Burns (2000)
15	Cariaco Basin	northern S. America dry (Fe/Ca, Ti/Ca)	?	Haug et al. (2001)
16	Cariaco Basin	↑ trade wind strength	↑ trade wind strength	Peterson et al. (1991); Lin et al. (1997)
17	Colombia	cool, wet (pollen)	−0–0.1°C, wet	Behling and Hooghiemstra (1998)
18	Colombia	−2–4°C, dry	−0–0.1°C, wet	Van der Hammen and Hooghiemstra (1995)
19	Columbia	−1–3°C, dry	−0–0.1°C, wet	Veer et al. (2000)
20	Haiti	Dry (ostracod $\delta^{18}\text{O}$ )	No response	Hodell et al. (1991)
21	Lake Chalco, Mexico	Dry (lake levels)	Wet?	Flores-Diaz (1986)
22	Costa Rica	−2–3°C (pollen)	−0–0.1°C?	Islebe et al. (1995)
23	Salar de Uyuni, Bolivia	Wet (lacustrine muds in ice core)	dry?	Baker et al. (2001)
24	Sajama, Bolivia	wet (ice core $\delta^{18}\text{O}$ and dust)	dry?	Thompson et al. (1998)
25	Huascarán, Peru	Cool and dry (ice core $\delta^{18}\text{O}$ and dust)	Cool, wet	Thompson et al. (1995)
African Precip Data				
26	Lake Victoria	Dry (lake levels)	Dry	Stager et al. (2002)
27	Ethiopia	Dry (lake levels)	Dry?	Gillespie et al. (1983); Gasse and Campo (1994)
28	Northern Sahara	Dry (carbonate $\delta^{18}\text{O}$ , mineralogy)	Dry	Gasse et al. (1990)
29	Western Sahara	Dry (lake levels)	Dry?	Gasse and Campo (1994)
30	Sahel/subequatorial Africa	Dry (lake levels)	Dry?	Gasse and Campo (1994)
31	Lake Bosumtwi (Ghana)	Dry (lake levels, pollen)	Wet?	Street-Perrott and Perrott (1990); Gasse and Campo (1994)
32	Lake Barombi Mbo (Cameroon)	Dry (pollen)	Wet?	Maley and Bernac (1998)
33	Kenya	Dry (bog organic carbon content)	Dry?	Street-Perrott and Perrott (1990)
34	Lake Malawi (East Africa)	Dry (biogenic silica fluxes)	Dry?	Johnson et al. (2002)
35	Rusaka Swamp (Burundi)	Dry (organic matter and pollen)	Dry	Bonnefille et al. (1995)
36	South Africa	No discernable change (pollen)	Dry?	Scott et al. (1995)

(Van der Hammen and Hooghiemstra 1995; Veer et al. 2000) indicate that the Younger Dryas was drier than the Bølling/Allerød. The history of rainfall in the Amazon basin is poorly known for the Bølling/Allerød–Younger Dryas transition. Several reconstructions based on marine sediments, however, suggest an increase in the strength of the northeast trade winds and a drying of northern South America and the Amazon basin during the Younger Dryas (Peterson et al. 1991; Lin et al. 1997; Arz et al. 1998; Maslin et al. 2000; Haug et al. 2001). The drying likely extended at least as far south as Huascarán, Peru, where Thompson et al. (1995) find a drying during the Younger Dryas based on ice-core reconstructions. In the Bolivian Altiplano, however, studies of two tropical ice cores suggest that conditions became wetter during the Younger Dryas Thompson et al. (1998); Baker et al. (2001).

In direct contrast to the studies from northern South America, our model results suggest a strong increase in precipitation (Fig. 9) and runoff (not shown), particularly in northeast Brazil, during a Younger Dryas-type event. The reason for this difference may involve the SST increase in the tropical Atlantic (Fig. 5). As discussed above, increased Atlantic SSTs are associated with increased rainfall in northeast Brazil, both in the model and in nature. SST reconstructions for the Younger Dryas do not uniformly demonstrate a warming in the tropical Atlantic. It is therefore possible that the discrepancy between the modeled and reconstructed South American precipitation results from differences in the direction and magnitude of SST change in the tropical Atlantic during the modeled and actual event. It is also possible that the southward shift of the ITCZ produced by the FW experiments does not dis-

**Fig. 12** Location and magnitude of SST and SAT changes associated with the Younger Dryas, as identified by paleoclimate proxies. Red tones indicate a warming, blue tones indicate a cooling. Units are °C. References (as in Table 2) are as follows: (1) Bard et al. (2000), (2) Calvo et al. (2001), (3) Zhao et al. (1995), (4) Kim et al. (2002), (5) Mulitza and Ruhlemann (2000), (6) Cohen et al. (1992), (7) Guilderson et al. (2001), (8) Hüls and Zahn (2000), (9) Rühlemann et al. (1999), (10) Arz et al. (1999), (11) Lea et al. (2003), (12) Flower and Kennett (1990)

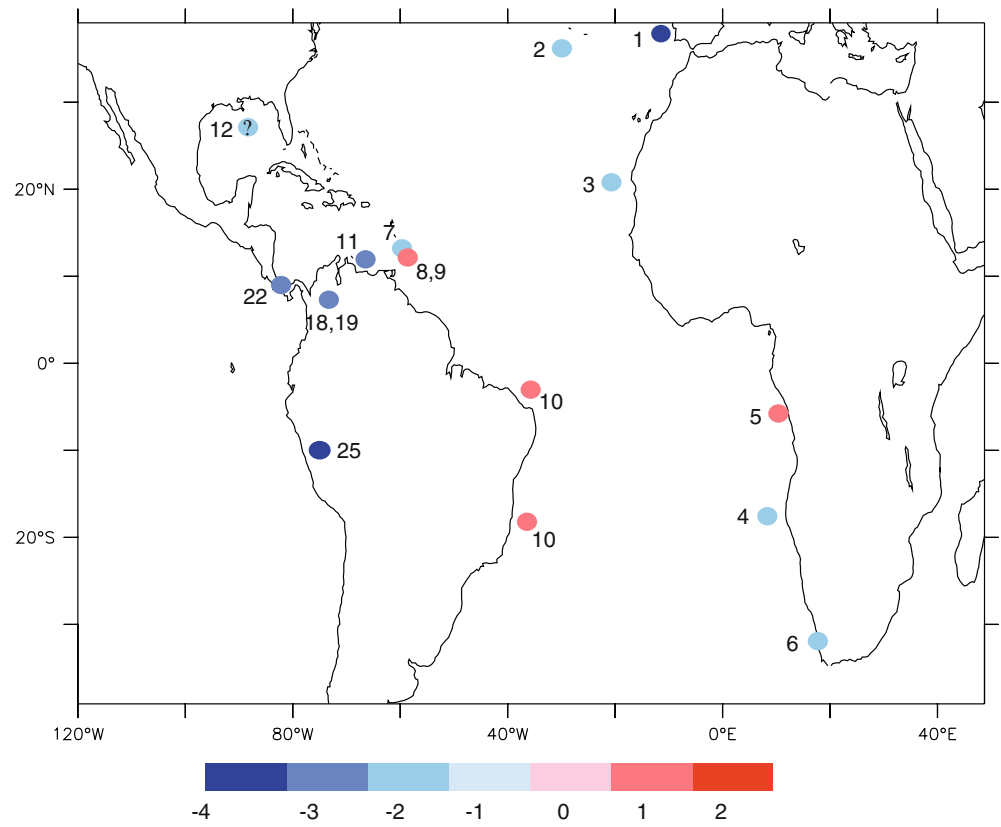
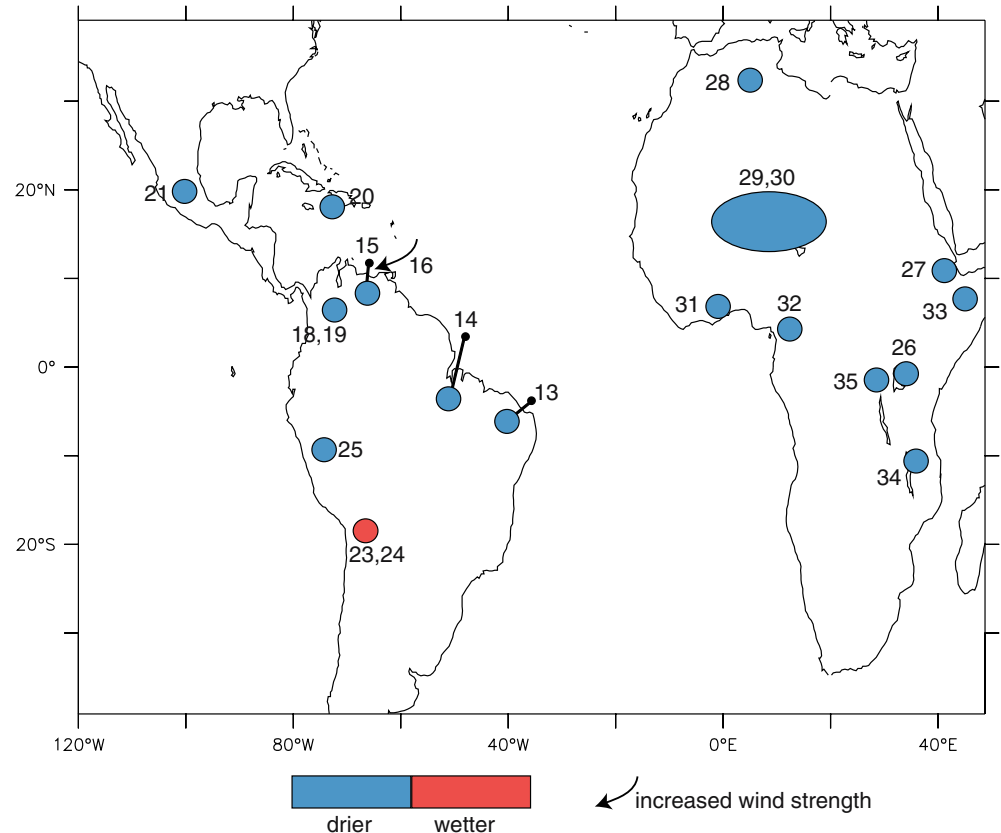


**Fig. 13** Precipitation changes associated with the Younger Dryas as identified by paleoclimate proxies. Red indicates increased precipitation, blue indicates decreased precipitation. The small black dots connected by lines to larger dots indicate that the authors have used a marine sediment core to infer moisture conditions on the continent. References (as in Table 2) are as follows: (13) Arz et al. (1998), (14) Maslin and Burns (2000), (15) Haug et al. (2001), (16) Peterson et al. (1991), Lin et al. (1997), (17) Behling and Hooghiemstra (1998), (18) Van der Hammen and Hooghiemstra (1995), (19) Veer et al. (2000), (20) Hodell et al. (1991), (21) Flores-Diaz (1986), (22) Islebe et al. (1995), (23) Baker et al. (2001), (24) Thompson et al. (1998), (25) Thompson et al. (1995)



place the ITCZ as far south as it may have been during the Younger Dryas.

Lake levels decreased throughout Africa during the Younger Dryas, which indicates that the majority of Africa experienced a drying during this time (Fig. 13; Street-Perrott and Perrott 1990; Gasse and Campo 1994; Bonnefille et al. 1995; Johnson et al. 2002; Stager et al. 2002). The evidence from lake levels is supported by pollen data from Lake Bosumtwi (Ghana; Street-Perrott and Perrott 1990; Gasse and Campo 1994), Lake Barombi (Cameroon; Maley and Bernac 1998), and the Rusaka Swamp (Burundi; Bonnefille et al. 1995), as well as biogenic silica data from Lake Malawi (East Africa; Johnson et al. 2002), organic carbon data from Kenya (Street-Perrott and Perrott 1990), and carbonate  $\delta^{18}\text{O}$  data from Algeria (Gasse et al. 1990). South Africa may be the exception to this widespread drying, as there is no clear evidence for changes in temperature or moisture during the Younger Dryas in this region (Scott et al. 1995).

While robust between the three experiments, the annually averaged precipitation change in the Sahel, equatorial, and subequatorial regions of Africa is small compared to the widespread drying indicated by the paleodata. Such small changes would not likely be detected in the paleoclimate record. The sense of the precipitation changes simulated by the model is in line with what the paleodata suggest; however, the magnitude of change recorded by the paleodata is much larger than the model's response. It is possible that the lack of interactive vegetation in the model could contribute to this discrepancy.

In summary, the modeled North Atlantic response is consistent with data from the Younger Dryas that suggest a cooling of North Atlantic SST and a reduction in the formation of NADW. Paleo-SST reconstructions for the tropical Atlantic suggest a heterogeneous response during the Younger Dryas. Three of the five sites within the region showing a warming during the FW experiments do exhibit a warming during the Younger Dryas. The two sites showing a Younger Dryas cooling lie within upwelling regions, which may complicate the paleoclimate data-model comparison. The warming predicted by the model is weaker than the SST reconstructions suggest for sites that underwent a warming during the Younger Dryas. Paleo-SAT data and the modeled SAT response agree in direction, but not in magnitude; i.e. the cooling of northern South America suggested by the model is weaker than that suggested by the paleoclimate data. The model response may also be affected by precipitation changes during the FW experiments that do not agree with paleoclimate data from South America. Both the model and paleoclimate data suggest that African precipitation decreased, but the modeled drying is weak compared to the changes indicated by the data. Paleoclimate data for South American precipitation changes during the Younger Dryas strongly disagree with the model response. However, this too may simply be the model not producing large

enough changes, as a farther southward shift of the ITCZ could induce a drying in NEB in the model. Thus, the freshwater forcing experiments performed for this study capture the direction, but not the magnitude, of change for several parameters (tropical Atlantic SST, African precipitation, and possibly the southward extent of the ITCZ) in the tropical Atlantic region.

The potential reasons why discrepancies exist between the model results and paleoclimate data fall into three main categories: model boundary conditions and experimental design, model limitations, and limitations of the paleoclimate data. The difference in boundary conditions between the model run (at modern boundary conditions) and the Younger Dryas could have a substantial impact on the ability of the model to simulate Younger Dryas-type climate change. As shown by Yin and Battisti (2001), ice sheets, which were likely present in some form during the Younger Dryas, act as amplifiers of subtle climate change by altering the course of storm tracks. In addition, land ice was shown by Chiang et al. (2003) to be the primary driver of the tropical Atlantic wind, precipitation, and SST response to Last Glacial Maximum boundary conditions. The presence of ice sheets during the Younger Dryas was also associated with sea levels on the order of 60 m lower than today (Fairbanks 1989). The mean climate state of the Younger Dryas was also likely to have been colder than the modern mean climate state. The sea-ice distribution, and the resulting feedbacks, was also most likely different during the Younger Dryas than it is in the model. While the model we used incorporates sea ice, a colder mean climate would enhance the sea ice-albedo feedback. If sea-ice growth in the model occurred under colder boundary conditions, the high-latitude response to FW forcing, and by extension the tropical Atlantic response, would be enhanced. It is also important to consider that, if, as suggested by Weaver et al. (2003), MWP1A originated from Antarctica and triggered the Bølling/Allerød, then the difference in climate between the Bølling/Allerød and the Younger Dryas could have been amplified relative to our "Younger Dryas" FW experiments that used modern-day boundary conditions. Finally, the duration of the forcing for the Younger Dryas was likely to have been much longer than the model freshwater forcing. Thus anomalies may have grown in strength throughout the Younger Dryas in such a way that they were unable to grow during the experiments. Despite the presumably large changes that these differing boundary conditions would have on our experiments, it is interesting to note that climate simulations that do impose Younger Dryas boundary conditions have also had difficulty simulating the changes inferred by paleoclimate data outside of the North Atlantic/Northern European region (Renssen 1997; Renssen and Isarin 1998; Renssen and Lautenschlager 2000).

Limitations of the model's climate feedbacks and architecture could also contribute to differences between the model response and paleoclimate data from the Younger Dryas. Evidence from both Greenland (GISP2)

and Antarctic (Taylor Dome) ice cores suggests that atmospheric methane levels dropped by about 200 ppbv at the Bøllng/Allerød–Younger Dryas transition (Brook et al. 2000). The additional negative radiative forcing associated with the decreased methane could have caused a cooling that was not represented with the model used in this study. In nature, vegetative feedback processes also have a significant effect on tropical climate. In mid-Holocene simulations, the terrestrial response to orbital forcing was amplified, thus becoming more realistic, when vegetation changes are included (Braconnot et al. 1999). Our model does not incorporate vegetation or atmospheric chemistry. Therefore, feedbacks associated with these processes do not contribute to the modeled response to freshwater forcing. It is also possible that an important climate forcing was not included in the experimental design. If millennial-scale variability is paced by variations in solar output, as was suggested by Bond et al. (2001), then the neglect of this component of the climate system may contribute to model–paleodata discrepancies. Precipitation patterns are relatively noisy in the model as well as in nature. While the model captures the general orographic features (and therefore rainfall patterns) associated with mountain ranges such as the Andes, it is unrealistic to expect that the simulated precipitation at a given location within the Andes will accurately reflect precipitation at that location in the real world. Similarly, the resolution of the model does not permit the accurate simulation of specialized environments, such as the Cariaco Basin. That the model's ITCZ generally overestimates precipitation over land may contribute to the discrepancies between precipitation patterns during the Younger Dryas and those that result from the freshwater forcing experiment. More specifically, the model may overestimate the precipitation increase in NEB and underestimate the drying of Africa as a result of the ITCZ's land bias. Finally, it is possible that the model's physics are not accurate enough to generate the responses indicated by the paleodata.

Uncertainties in the interpretation of paleoclimatic data could also contribute to model–paleodata differences. In terms of age control, there are uncertainties in both the measurement of  $^{14}\text{C}$  and in the estimation of the reservoir age of a marine system through time. Furthermore, recent evidence suggests that alkenones, from which SST can be derived, are often several thousand years older than foraminifera from the same depth horizon (Ohkouchi et al. 2002). The proxy data itself is also subject to some uncertainty. For example, there is a strong seasonality to alkenone production; therefore alkenone-derived SSTs may reflect the temperature only during one season. Furthermore, given that alkenone-producing coccolithophorids do not live exactly at the sea surface, alkenone temperatures may be recording slightly deeper, and therefore, colder temperatures. Depending upon the specific depth habitat of the coccolithophorids, this may partially explain why alkenone-based SST reconstructions record a Younger

Dryas warming closer in magnitude to the FW temperature anomalies at thermocline depths.

### 3.2.2 Intra-model comparison

Despite differences in computer systems, starting values of North Atlantic MOC, and control runs, the results described in this paper are robust for all three of the individual FW experiments. In order to assess the robustness of the responses, we have compared the response of each of the three FW experiments using ten indices (Fig. 14). The indices we have chosen are: North Atlantic MOC, SAT in the region south of Greenland, SAT over the Barents Sea, tropical Atlantic SST, ANN, DJF, and JJA precipitation in South America and Africa. All comparisons were made for the last 20–25 years of each experiment. The mean and range of the anomalies for each of these indices are shown in Fig. 15.

For each FW experiment, the overall decrease in North Atlantic MOC was 8–9 Sv, a ~40% decrease from the original value. The reduction for each experiment occurred within two decades. All three experiments also demonstrate multidecadal variability of the North Atlantic MOC that has a similar timescale, but a lower magnitude, to the variability observed in the control runs.

SAT anomalies south of Greenland vary by about 1°C between the three FW experiments, with a mean cooling of about 5°C. The range in SAT anomalies for the Barents Sea region is greater: about 2°C, with a mean value of 2°C. Despite the broad range of temperature anomalies in the Barents Sea, all three experiments show a warming in this region. Tropical Atlantic SST anomalies vary by less than 0.05°C between the three runs. All three experiments show a warming of ~2°C for the region shown in Fig. 14.

Precipitation anomalies for all three FW experiments show an increase in South American precipitation during both the summer (JJA) and the winter (DJF), as well as on an annual basis. The largest anomaly, DJF, also has the greatest range in magnitude. African precipitation in all three experiments exhibits a slight decrease. Despite the mild nature of this drying, it is robust for both the annual average as well as for DJF and JJA.

### 3.2.3 Comparison with simulations by other models

Several modeling groups have performed experiments similar to those of this study using coupled ocean–atmosphere GCMs. Descriptions of the experiments we will consider in this section (Manabe and Stouffer 1997; Schiller et al. 1997; Rind et al. 2001; Vellinga and Wood 2002) can be found in Table 3. The deepwater response obtained with the FW experiments is qualitatively similar to those of other freshwater forcing studies, which all show decreases in North Atlantic MOC of 30–50% ~100 years after the forcing is applied. All of the models also show maximum cooling in the North Atlantic region.

**Fig. 14** Indices for intra-model comparison

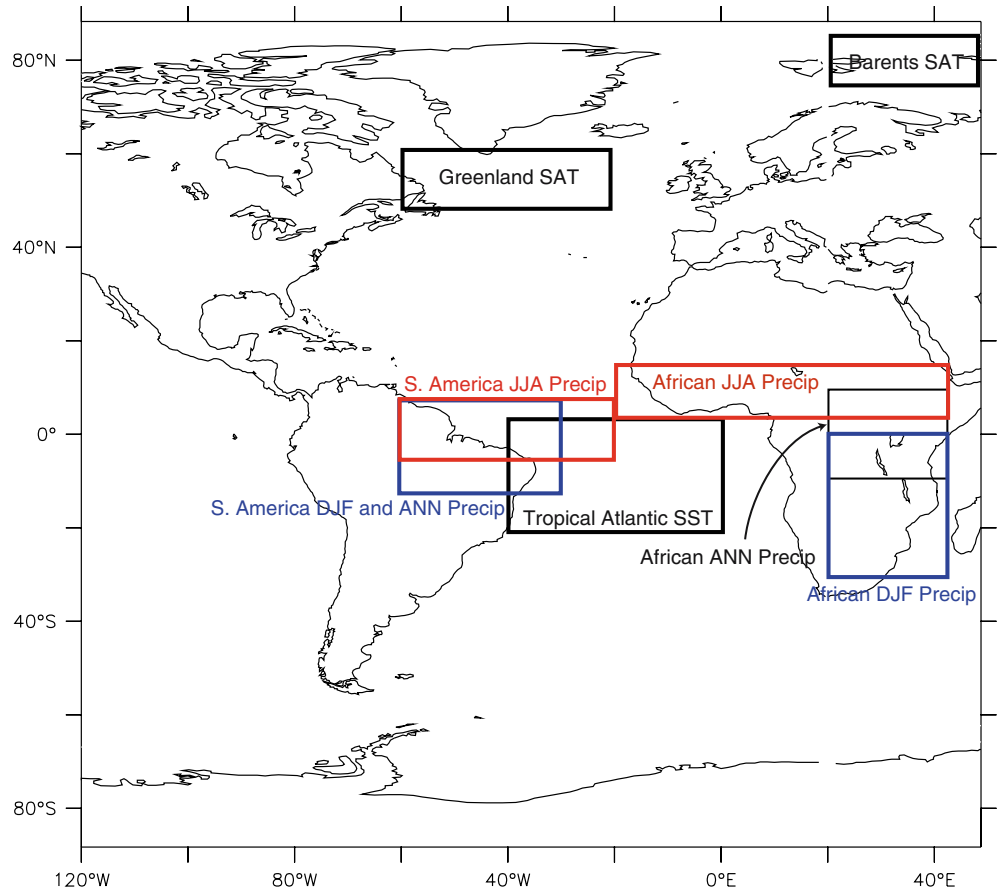
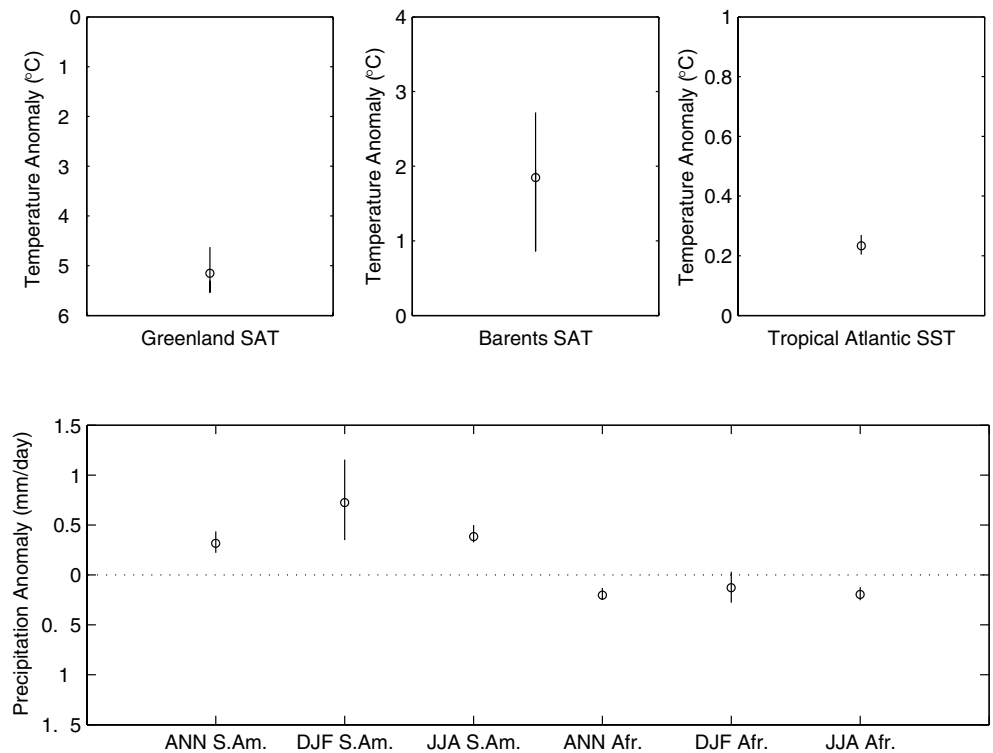


**Fig. 15** Variability of the responses of the three FW experiments for various indices shown in Fig. 14. The ensemble mean anomaly is shown as an open circle, and the range of anomalies is shown as a bar through the circle



In the tropical Atlantic, the SAT response of the R30 model is similar to that of Schiller et al. (1997) and Vellinga and Wood (2002), who found a warming of up to 3.0°C over much of the tropical Atlantic Ocean. Rind et al. (2001) also find a warming response in experiments with greater freshwater forcing (32× St. Lawrence) or weaker control run thermohaline circulation (8× St. Lawrence with FLUX control run). Similar to our findings, Rind et al. (2001) document a pattern of cooling (0.1–0.5°C) over South America after 160 years. The SAT anomalies generated during the Manabe and Stouffer (1997) experiment show a widespread warming over the entire tropical Atlantic region with only isolated patches of slight cooling over eastern South America. Over Africa, the studies discussed here, with the exception of Vellinga and Wood (2002) show a patchy warming of 0.1–2.5°C.

The tropical Atlantic precipitation anomalies observed in these experiments are very similar to those observed by Manabe and Stouffer (1997) in both magnitude and location for NEB and Africa Schiller et al. (1997) and Vellinga and Wood (2002) also find large (2 mm day<sup>-1</sup>) increases in precipitation in northeast Brazil, although their anomalies are shifted further offshore than the anomaly found in this study. Furthermore, both Schiller et al. (1997) and Vellinga and Wood (2002) document strong drying over northwestern half of South America that we do not find here. The magnitude and spatial pattern of drying over Africa documented by Schiller et al. (1997) and our study are similar, while Vellinga and Wood (2002) find patchy increases in precipitation. Given the noisy nature of precipitation in models, we can consider Schiller et al. (1997) and our study to be in relatively good agreement with one another. With the exception of Rind et al. (2001), all of the model experiments considered here show a southward shift in the ITCZ in response to North Atlantic freshwater forcing.

In contrast, Rind et al. (2001) find little change in the precipitation in South America and an increase in precipitation of 0.1–0.5 mm day<sup>-1</sup> in Eastern Africa. However, the precipitation response they find using a much greater freshwater forcing rate (0.53 Sv, 32× St. Lawrence) is generally more consistent with the results of this study.

In summary, there are several responses to North Atlantic freshwater forcing for which the majority of models concur. The value for SAT cooling in the North

Atlantic seems to be converging on ~8°C. While some models show more or less cooling, the direction of the anomaly (i.e. cooling) is consistent. All of the models discussed here show some degree of warming of tropical Atlantic SAT, and four out of the five models show an increase in precipitation in Northeast Brazil. Precipitation changes over Africa are less consistent between models, with three models showing decreased African precipitation and two showing patchy increases. The differences in the magnitude of the modeled responses could be caused by a number of factors, including model architecture, different forcings, and different initial conditions. The forthcoming results of the CMIP (Coupled Model Intercomparison Project) experiments, in which many modeling groups have prescribed the same freshwater forcing, should further elucidate the relationship between model architecture and experimental outcome.

## 4 Conclusions

Using a coupled OAGCM, we have examined the response of the tropical Atlantic to a North Atlantic freshwater forcing event. A three-member ensemble of experiments shows that, in response to this forcing, the climate state of the Atlantic is significantly changed. The largest responses occur in the North Atlantic, where MOC decreases by 40% and SATs cool by up to ~8°C. Responses in the tropical Atlantic are more subtle. The increased meridional temperature gradient induced by the high latitude cooling causes the northern hemisphere extratropics to demand more heat from the tropics. The ITCZ therefore shifts southward and the Northeast trade winds increase in strength. As a result of the change in the winds and the position of the ITCZ, precipitation patterns throughout the Atlantic basin change. Specifically, precipitation north of 10°N decreases, while precipitation in Northeast Brazil increases substantially and Africa undergoes a mild drying. The changes in precipitation over the continents alter the amount of latent versus sensible heating of the land. Consequently, in general, South America cools while Africa warms.

The strongest tropical Atlantic temperature response occurs in the thermocline, where temperatures warm by up to 4.5°C. This warming, which was noted in previous studies (e.g. Manabe and Stouffer 1997), results from a combination of a decrease in the strength of northward-

**Table 3** Other freshwater forcing experiments discussed in this study

Authors	Model	Forcing applied	Duration	Initial MOC	Recovery time
This study	GFDL R30	0.1 Sv	100 years	24 Sv	50 years
Manabe and stouffer (1997)	GFDL R15	0.1 Sv	500 years	18 Sv	250 years
Rind et al. (2001) (Run LTC1)	GISS	0.15 Sv in N. Atlantic + inputs elsewhere	160 years	20 Sv (and decreasing)	No recovery
Schiller et al. (1997)	ECHAM3	Linear increase 0–0.625 Sv	250 years	18 Sv	120 years
Vellinga and Wood (2002)	HadCM3	2 psu decrease in N. Atlantic	0	20 Sv	120 years

flowing currents in the surface and thermocline layers. Warm water is thus allowed to remain in the tropics without being exported to the north or replenished by colder waters from below. These effects occur as a result of a decreased need for surface-water compensation of waters exported from the North Atlantic via deep-water formation. It is probable that the weak (0.2–0.3°C) warming of tropical Atlantic SSTs reflects a surface damping of the response at depth.

Comparison of the model's response to paleoclimate data from the Younger Dryas reveals that, for many parameters, the freshwater forcing experiments capture the direction but underestimate the magnitude of changes indicated by the paleoclimate data. An example of this is the moderate drying of Africa in the model compared to the widespread drying indicated by a variety of aridity proxies for the Younger Dryas. These differences could result from a number of factors, the most notable of which is that the model was run using modern-day boundary conditions, whereas the boundary conditions for the Younger Dryas were likely to have been very different.

Analysis of the three ensemble members shows that, despite slight differences in initial MOC conditions, computer systems, and control runs, the responses discussed above are robust in each member of the ensemble. In no case does the range of responses exhibited by the ensemble members change the direction of the response.

The results of this study allowed us to identify a number of responses to freshwater forcing experiments that are consistent across a range of models and experimental conditions. These robust responses include an 8°C cooling of North Atlantic SAT, a moderate warming of tropical Atlantic SST and SAT, an increase in precipitation in Northeast Brazil, and, to a lesser extent, decreased precipitation in Africa. While the North Atlantic cooling and decreased African precipitation are in line with the paleoclimate data for the Younger Dryas, the widespread warming of tropical SST and SAT and the increased Northeast Brazil precipitation are not. The latter observations suggest that one or more of the following problems exist: (1) Multiple models are unable to simulate a Younger Dryas-type event or (2) The paleoclimate data, which come from a wide variety of proxies, are flawed. We suspect that the primary reason for discrepancies between the models and the paleoclimate data is that there are numerous forcings associated with the Younger Dryas, such as land ice and vegetative feedbacks that were not incorporated into many models, including the model used in this study. In order to investigate this possibility, additional freshwater forcing experiments, particularly those with Bølling/Allerød or Younger Dryas boundary conditions should be performed. In addition, the pattern of SST changes during the Younger Dryas will become clearer as more and more high-resolution SST reconstructions are carried out. Further investigation of millennial-scale variability during the Holocene may provide a more

appropriate analog to freshwater forcing experiments, such as this one, performed with modern-day boundary conditions. Despite differences between paleoclimate reconstructions of the Younger Dryas and the modeled response to freshwater forcing, our results suggest that abrupt climate changes in the high latitudes can have a significant effect on tropical climate.

**Acknowledgements** We would like to thank Ruediger Gerdes, Rong Zhang, Delia Oppo, and two anonymous reviewers for thoughtful discussions and reviews of this manuscript. This work was funded in part by a WHOI Watson Fellowship (to kad).

## References

- Altabet MA, Higgenson MJ, Murray DW (2002) The effect of millennial-scale changes in Arabian Sea denitrification on atmospheric CO<sub>2</sub>. *Nature* 415:159–162
- Ammann B, Eicher U, Gaiullard MJ, Haeberli W, Lister G, Lotter AF, Maisch M, Niessen F, Schluchter CH, Wolfarth B (1994) The Würmian late-glacial in lowland Switzerland. *J Quaternary Sci* 9:119–127
- Arz HW, Pätzold JP, Wefer G (1998) Correlated millennial-scale changes in surface hydrography and terrigenous sediment yield inferred from last glacial marine deposits off Northeastern Brazil. *Quaternary Res* 50:157–166
- Arz HW, Pätzold J, Wefer G (1999) The deglacial history of the western tropical Atlantic as inferred from high resolution stable isotope records off northeastern Brazil. *Earth Planet Sci Lett* 167:105–117
- Baker PA, Rigsby CA, Seltzer GO, Frisk SC, Lowenstein TK, Bacher NP, Veliz C (2001) Tropical climate changes at millennial and orbital timescales on the Bolivian Altiplano. *Nature* 409:698–701
- Bard E, Rostek F, Turon JL, Gendreau S (2000) Hydrological impact of Heinrich Events in the Subtropical North Atlantic. *Science* 289:1321–1324
- Behl RJ, Kennett JP (1996) Brief interstadial events in the Santa Barbara basin, NE Pacific, during the past 60 kyr. *Nature* 379:243–246
- Behling H, Hooghiemstra H (1998) Late Quaternary palaeoecology and palaeoclimatology from pollen records of the savannas of the Llanos Orientales in Colombia. *Palaeogeogr Palaeoclim Palaeoecol* 139:251–267
- Bond G, Showers W, Cheseby M, Lotti R, Almasi P, deMenocal P, Priore P, Cullen H, Hajdas I, Bonani G (1997) A pervasive millennial-scale cycle in North Atlantic Holocene and glacial climates. *Science* 278:1257–1266
- Bond G, Kromer B, Beer J, Muscheler R, Evans MN, Showers W, Hoffmann S, Lotti-Bond R, Hajdas I, Bonani G (2001) Persistent solar influence on North Atlantic climate during the Holocene. *Science* 294:2130–2136
- Bonnefille R, Riollet G, Buchet G, Icole M, Lafont R, Arnold M, Jolly D (1995) Glacial/interglacial record from intertropical Africa, high resolution pollen and carbon data at Rusaka Burundi. *Quaternary Sci Rev* 14:917–936
- Boyle EA, Keigwin LD (1987) North Atlantic thermohaline circulation during the last 20,000 years linked to high latitude surface temperature. *Nature* 330:35–40
- Braconnot B, Joussaume S, Marti O, de Noblet N (1999) Synergistic feedbacks from ocean and vegetation on the African monsoon response to mid-Holocene insolation. *Geophys Res Lett* 26:2481–2484
- Broecker WS (1995) *The glacial world according to Wally*. Eldigio Press, Palisades
- Broecker WS, Peteet D, Rind D (1985) Does the ocean-atmosphere system have more than one stable mode of operation?. *Nature* 315:21–25

- Broecker WS, Andree M, Wolli W, Oeschger W, Bonani G, Kennett J, Peteet DA (1988) A case in support of a meltwater diversion as the trigger for the onset of the Younger Dryas. *Paleoceanography* 3:1–9
- Brook EJ, Harder S, Severinghaus J, Steig EJ, Sucher CM (2000) On the origin and timing of rapid changes in atmospheric methane during the last glacial period. *Global Biogeochem Cycles* 14:559–572
- Calvo E, Villanueva J, Grimalt JO, Boelaert A, Labeyrie L (2001) New insights into the glacial latitudinal temperature gradients in the North Atlantic. Results from U37k' sea-surface temperatures and terrigenous inputs. *Earth Planet Sci Lett* 188:509–519
- Cane MA (1998) A role for the tropical Pacific. *Science* 282:59–61
- Chappellaz J, Blunier T, Raynaud D, Barnola JM, Schwander J, Stauffer B (1993) Synchronous changes in atmospheric CH<sub>4</sub> Greenland climate between 40 and 8 kyr BP. *Nature* 366:443–445
- Chiang JCH, Biasutti M, Battisti DS (2003) Sensitivity of the Atlantic Intertropical Convergence Zone to Last Glacial Maximum boundary conditions. *Paleoceanography* 18:10.1029/2003PA000916
- Clement AC, Cane MA (1999) A role for the tropical Pacific coupled ocean-atmosphere system on Milankovitch and millennial timescales part I: a modeling study of tropical Pacific variability. In: Clark PU, Webb RS, Keigwin LD (eds) *Mechanisms of Global Climate Change on Millennial Timescales*, vol. 112. American Geophysical Union, Washington DC
- Clement AC, Cane MA, Seager R (2001) An orbitally driven tropical source for abrupt climate change. *J Climate* 14:2369–2375
- Cohen AL, Parkington JE, Brundrit JB, Van Der Merwe NJ (1992) A Holocene marine climate record in mollusc shells from the southwest African coast. *Quaternary Res* 38:379–385
- Cubasch U, Meehl GA, Boer GR, Stouffer RJ, Dix M, Noda A, Senior CA, Raper S, Yap KS, Abe-Ouchi A, Brinkop S, Claussen M, Collins M, Evans J, Fischer-Bruns L, Flato G, Fyfe JC, Ganopolski A, Gregory JM, Hu Z-Z, Joos F, Knutson T, Knutti R, Landsea C, Mearns L, Milly C, Mitchell JFB, Nozawa T, Paeth H, Sausen RJ, Smith S, Stocker T, Timmerman A, Ulbrich U, Weaver A, Wegner J, Whetton P, Wigley T, Winton M, Zwiers F (2001) Projections of future climate change. In: Houghton JT, Ding Y, Griggs DJ, Noguer M, van der Linden PJ, Dai X, Maskell K, Johnson CA (eds) *Climate change 2001: The scientific basis*. Cambridge University Press, Cambridge, pp 555–582
- Curry WB, Marchitto T, McManus JF, Oppo DW, Laarkamp KL (1999) Millennial-scale changes in ventilation of the thermocline, intermediate, and deep waters of the glacial North Atlantic. In: Clark PU, Webb RS, Keigwin LD (eds) *Mechanisms of global climate change at millennial timescales*, vol. 112. American Geophysical Union, Washington DC, pp 59–78
- Dansgaard W, White JWC, Johnsen SJ (1989) The abrupt termination of the Younger Dryas climate event. *Nature* 339:532–533
- deBeaulieu J-L, Andrieu V, Lowe JJ, Ponel P, Reille M (1994) The Weichselian late-glacial in southwestern Europe Iberian Peninsula, Pyrenees, Massif Central, Northern Appenines. *J Quaternary Sci* 9:101–108
- Delworth TL, Mann ME (2000) Observed and simulated multidecadal variability in the Northern Hemisphere. *Clim Dyn* 16:661–676
- Delworth T, Manabe S, Stouffer RJ (1993) Interdecadal variations of the thermohaline circulation in a coupled ocean-atmosphere model. *J Climate* 6:1993–2011
- Delworth TL, Manabe S, Stouffer RJ (1997) Multidecadal climate variability in the Greenland Sea and surrounding regions: a coupled model simulation. *Geophys Res Lett* 24:257–260
- Delworth TL, Stouffer RJ, Dixon KW, Spelman MJ, Knutson TR, Broccoli AJ, Kushner PJ, Wetherald RT (2002) Simulation of climate variability and change by the GFDL R30 coupled climate model. *Clim Dyn* 19:555–574
- Deser C, Blackmon ML (1995) On the relationship between tropical and North Pacific sea-surface temperature variations. *J Climate* 8:1677–1680
- Dickson RR, Brown J (1994) The production of North Atlantic deep water: sources, rates, and pathways. *Geophys J Res* 99:12319–12341
- Dong BW, Sutton RT (2002) Adjustment of the coupled ocean-atmosphere system to a sudden change the thermohaline circulation. *Geophys Res Lett* 29:10.1029/2002GL015229
- Fairbanks RJ (1989) A 17,000-year glacio-eustatic sea level record: influence of glacial melting rates on the Younger dryas event and deep-ocean circulation. *Nature* 342:637–642
- Fairbanks RJ (1990) The age and origin of the Younger Dryas Climate Event in Greenland ice cores. *Paleoceanography* 5:937–948
- Flores-Diaz A (1986) In: Lorenzo JL, Mirambell M (eds) *Tlapacoya: 35,000 Años de Historia del Lago de Chalco* Instituto Nacional de Antropología e Historia, Mexico City, pp 109–156
- Flower BP, Kennett JP (1990) The Younger Dryas cool episode in the Gulf of Mexico. *Paleoceanography* 5:949–961
- Folland CK, Colman AW, Rowell DP, Davey MK (2001) Predictability of Northeast Brazil rainfall and real-time forecast skill 1987–98. *J Climate* 14:1937–1958
- Gasse F, Van Campo E (1994) Abrupt post-glacial climate events in West Asia and North Africa monsoon domains. *Earth Planet Sci Lett* 126:435–456
- Gasse F, Tehet R, Durand A, Gilbert E, Fontes JC (1990) The arid-humid transition in the Sahara and the Sahel during the last deglaciation. *Nature* 346:141–146
- Gillespie R, Street-Perrott FA, Switsur R (1983) Post-glacial arid episodes in Ethiopia have implications for climate prediction. *Nature* 306:680–683
- Guilderson TP, Fairbanks RG, Rubenstone JL (2001) Tropical Atlantic coral oxygen isotopes: glacial-interglacial sea-surface temperatures and climate change. *Marine Geol* 172:75–89
- Hastenrath S, Heller L (1977) Dynamics of climate hazards in Northeast Brazil. *Quart J Roy Meteor Soc* 103:77–92
- Haug GH, Hughen KA, Sigman DM, Peterson LC, Röhl U (2001) Southward migration of the intertropical convergence zone through the Holocene. *Science* 293:1304–1308
- Hodell DA, Curtis JH, Jones GA, Higuera-Gundy A, Brenner M, Binford MV, Dorsey KT (1991) Reconstruction of Caribbean climate change over the past 10,500 years. *Nature* 352:790–793
- Hüls M, Zahn R (2000) Millennial-scale sea surface temperature variability in the western tropical North Atlantic from planktonic foraminiferal census counts. *Paleoceanography* 15:659–678
- Islebe GA, Hooghiemstra H, van der Borg K (1995) A cooling event during the Younger Dryas Chron in Costa Rica. *Palaeogeogr Palaeoclim Palaeoecol* 117:73–80
- Johnson TC, Brown ET, McManus J, Barry S, Barker P, Gasse F (2002) A high-resolution paleoclimatic record spanning the past 25,000 years in southern East Africa. *Science* 296:113–114
- Keigwin LD, Jones GA, Lehman SJ, Boyle EA (1991) Deglacial meltwater discharge North Atlantic deep circulation and abrupt climate change. *Geophys J Res* 96:16811–16286
- Keigwin LD, Curry WB, Lehman SJ, Johnson GS (1994) The role of the deep ocean in North Atlantic climate change between 70 and 130 kyr ago. *Nature* 371:323–326
- Kim JH, Schneider RR, Müller PJ, Wefer G (2002) Interhemispheric comparison of deglacial sea-surface temperature patterns in Atlantic eastern boundary currents. *Earth Planet Sci Lett* 194:383–393
- Klein SA, Soden BJ, Lau N-C (1999) Remote sea-surface temperature variations during ENSO: evidence for a tropical atmospheric bridge. *J Climate* 12:917–932
- Kroon D, Austin WEN, Chapman MR, Ganssen GM (1997) Deglacial surface circulation changes in the northeastern Atlantic: temperature and salinity records off NW Scotland on a century scale. *Paleoceanography* 12:755–763
- Lau N-C (1997) Interaction between global SST anomalies and the midlatitude atmospheric circulation. *B Am Meteorol Soc* 78:21–33

- Lau N-C, Nath MJ (1996) The role of the “atmospheric bridge” in linking tropical Pacific ENSO events to extratropical SST anomalies. *J Climate* 9:2036–2057
- Lea DW, Pak DK, Peterson LC, Hughen KA (2003) Synchronicity of tropical and high-latitude Atlantic temperatures over the last glacial termination. *Science* 301:1361–1364
- Levitus S, Boyer T (1994) *World Ocean Atlas 1994*, vol. 4: Temperature vol. 13 of NOAA Atlas NESDIS US. Government Printing Office, Washington DC
- Licciardi JM, Teller JT, Clark PU (1999) Freshwater routing by the Laurentide ice sheet during the last deglaciation. In: Clark PU, Webb RS, Keigwin LD (eds) *Mechanisms of global climate change on millennial timescales*, vol. 112. American Geophysical Union, Washington DC, pp 177–201
- Lin HL, Peterson LC, Overpeck JT, Trumbore SE, and Murray DW (1997) Late Quaternary climate change from  $\delta^{18}\text{O}$  records of multiple species of planktonic foraminifera: High-resolution records from the anoxic Cariaco Basin, Venezuela. *Paleoceanography* 12:415–427
- MacAyeal DR (1993) Binge/purge oscillations of the Laurentide ice sheets as a cause of the North Atlantic’s Heinrich events. *Paleoceanography* 8:775–784
- Maley J, Brenac P (1998) Vegetation dynamics, palaeoenvironments and climatic changes in the forests of western Cameroon during the last 28,000 years B.P. *Rev Palaeobot Palynol* 99:157–187
- Manabe S, Stouffer RJ (1995) Simulation of abrupt climate change induced by freshwater input to the North Atlantic Ocean. *Nature* 378:165–167
- Manabe S, Stouffer RJ (1997) Coupled ocean-atmosphere model response to freshwater input: comparison to the Younger Dryas event. *Paleoceanography* 12:321–336
- Manabe S, Stouffer RJ, Spelman MJ, Bryan K (1991) Transient responses of a coupled ocean-atmosphere model to gradual changes of atmospheric  $\text{CO}_2$  part I: annual mean response. *J Climate* 4:785–818
- Marchitto TM, Curry WB (1998) Millennial-scale changes in North Atlantic circulation since the last glaciation. *Nature* 393:557–661
- Markham CG, McLain DR (1977) Sea-surface temperature related to rain in Ceara, northeastern Brazil. *Nature* 265:320–323
- Maslin MA, Burns SJ (2000) Reconstruction of the Amazon Basin effective moisture availability over the past 14,000 years. *Science* 290:2285–2287
- Mechoso CR, Lyons SW, Spahr JA (1990) The impact of sea-surface temperature anomalies on the rainfall over northeast Brazil. *J Climate* 3:812–826
- Moura AD, Shukla J (1981) On the dynamics of droughts in Northeast Brazil: observations, theory, and numerical experiments with a general circulation model. *J Atmos Sci* 38:2653–2675
- Mulitza S, Rühlemann CR (2000) African monsoonal precipitation modulated by interhemispheric temperature gradients. *Quaternary Res* 53:270–274
- Nicholson SE (2000) The nature of rainfall variability over Africa on time scales of decades to millennia. *Global Planet Change* 26:137–158
- Ohkouchi N, Eglinton TI, Keigwin LD, Hayes JM (2002) Spatial and temporal offsets between proxy records in a sediment drift. *Science* 298:1224–1227
- Oppo DW, Lehman SJ (1995) Suborbital timescale variations of North Atlantic Deep Water during the past 135,000 years. *Paleoceanography* 10:901–910
- Pacanowski R, Dixon K, Rosati A (1991) *The GFDL Modular Ocean Model users guide version 1*. GFDL Ocean Group Technical Report 2
- Peagle JN, Mo KC (2002) Linkages between summer rainfall variability over South America and sea-surface temperature anomalies. *J Climate* 15:1389–1407
- Peterson LC, Overpeck JT, Kipp NG, Imbrie J (1991) A high-resolution late quaternary upwelling record from the anoxic Cariaco Basin, Venezuela. *Paleoceanography* 6:99–119
- Peterson LC, Haug GH, Hughen KA, Röhl U (2000) Rapid changes in the hydrologic cycle of the tropical Atlantic during the last glacial. *Science* 290:1947–1950
- Pezzi P, Cavalcanti IFA (2001) The relative importance of ENSO and tropical Atlantic sea-surface temperature anomalies for seasonal precipitation over South America: a numerical study. *Clim Dyn* 17:205–212
- Rahmstorf S (1995) Bifurcations of the Atlantic thermohaline circulation in response to changes in the hydrological cycle. *Nature* 378:145–149
- Renssen H (1997) The global response to ounger Dryas boundary conditions in an AGCM simulation. *Clim Dyn* 13:587–599
- Renssen H, Isarin RFB (1998) Surface temperature in NW Europe during the Younger Dryas: AGCM simulation compared with temperature reconstructions. *Clim Dyn* 14:33–44
- Renssen H, Lautenschlager M (2000) The effect of vegetation in a climate model simulation of the Younger Dryas. *Global Planet Change* 26:423–443
- Rind D, de Menocal P, Russell G, Sheth S, Collins D, Schmidt G, Teller J (2001) Effects of glacial meltwater in the GISS coupled atmosphere-ocean model 1. North Atlantic Deep Water response. *J Geophys Res* 106:27325–27353
- Rosell-Mele A, Koc N (1997) Paleoclimatic significance of the stratigraphic occurrence of photosynthetic biomarker pigments in the Nordic seas. *Geology* 25:49–52
- Rühlemann C, Mulitza S, Muller PJ, Wefer G, Zahn R (1999) Warming of the tropical Atlantic Ocean and slowdown of the thermohaline circulation during the last deglaciation. *Nature* 402:511–514
- Schiller A, Mikolajewicz U, and Voss A (1997) The stability of the North Atlantic thermohaline circulation in a coupled ocean-atmosphere general circulation model. *Clim Dyn* 13:325–347
- Schmittner A, Appenzeller C, Stocker TF Enhanced Atlantic freshwater export during an El Niño. *Geophys Res Lett* 27:1163–1166
- Scott L, Steenkamp M, Beaumont PB (1995) Palaeoenvironmental conditions in South Africa at the Pleistocene–Holocene transition. *Quaternary Sci Rev* 14:937–947
- Smethie WJ Jr, Fine RA (2001) Rates of North Atlantic deep water formation calculated from chlorofluorocarbon inventories. *Deep Sea Res Part I* 48:189–215
- Stager JC, Mayewski PA, Meeker LD (2002) Cooling cycles, Heinrich event 1, and the dessication of Lake Victoria. *Palaeogeogr Palaeoclim Palaeoecol* 183:169–178
- Street-Perrott FA, Perrott RA (1990) Abrupt climate fluctuations in the tropics: the influence of Atlantic Ocean circulation. *Nature* 343:607–610
- Thompson LG, Mosley-Thompson E, Davis ME, Lin P-N, Henderson KA, Cole-Dai J, Bolzan JF, Liu KB (1995) Late glacial stage and Holocene tropical ice core records from Huascarán, Peru. *Science* 269:46–50
- Thompson LG, Davis ME, Mosley-Thompson E, Sowers TA, Henderson KA, Zagorodov VS, Lin P-N, Mikhalevko VN, Campen RK, Bolzan JF, Cole-Dai J, Francou B (1998) A 25,000-year tropical climate history from Bolivian ice cores. *Science* 282:1858–1864
- Uvo CB, Repelli CA, Zebiak SE, Kushnir Y (1998) The relationship between tropical Pacific and Atlantic SST and Northeast Brazil monthly precipitation. *J Climate* 11:551–562
- Van der Hammen T, Hooghiemstra H (1995) The El Abra stadial, a Younger Dryas equivalent in Colombia. *Quaternary Sci Rev* 14:841–851
- Veer R, Islebe GA, Hooghiemstra H (2000) Climatic change during the Younger Dryas chron in northern South America: a test of the evidence. *Quaternary Sci Rev* 19:1821–1835
- Vellinga M, Wood RA (2002) Global climatic impacts of a collapse of the Atlantic thermohaline circulation. *Climatic Change* 54:251–267
- Venegas SA, Mysak LA (2000) Is there a dominant timescale of natural climate variability in the Arctic? *J Climate* 13:3412–3434
- Vidal L, Labeyrie L, Cortijo E, Arnold M, Duplessy JC, Michel E, Becque S, van Weering TCE (1997) Evidence for changes in the

- North Atlantic deep water linked to meltwater surges during Heinrich events. *Earth Planet Sci Lett* 146:13–27
- Waliser DE, Gautier C (1993) A satellite-derived climatology of the ITCZ. *J Climate* 6:2162–2174
- Walker MJC, Bohncke SJP, Coope GR, O'Connell M, Usinger H, Verbruggen C (1994) The Devensian/Weichselian late-glacial in northwest Europe (Ireland, Britain, north Belgium, the Netherlands, northwest Germany). *J Quaternary Sci* 9:109–118
- Wallace JM, Gutzler DS (1981) Teleconnections in the geopotential height field during the Northern Hemisphere winter. *Mon Weather Rev* 115:784–812
- Wang YJ, Cheng H, Edwards RH, An ZS, Wu JY, Shen C-C, Dorale JA (2001) A high-resolution absolute-dated Late Pleistocene monsoon record from Hulu Cave, China. *Science* 294:2345–2348
- Weaver AJ, Saenko OA, Clark PU, Mitrovica JX (2003) Meltwater pulse 1A from Antarctica as a trigger of the Bølling–Allerød warm interval. *Science* 299:1709–1713
- Xie P, Arkin PA (1997) Global precipitation: a 17-year monthly analysis based on gauge observations, satellite estimates, and numerical model output. *Bull. Am Meteorol Soc* 78:2539–2558
- Yin JH, Battisti DS (2001) The importance of tropical sea-surface temperature patterns in simulations of the Last Glacial Maximum climate. *J Climate* 14:565–581
- Zahn R, Schonfield J, Kudrass H-R, Park M-H, Erlenkeuser H, Grootes P (1997) Thermohaline instability in the North Atlantic during meltwater events: stable isotope and ice-rafted detritus records from core S075-26KL, Portuguese margin. *Paleoceanography* 12:696–710
- Zhao M, Beveridge NAS, Shackleton NJ, Sarnthein M, Eglinton G (1995) Molecular stratigraphy of cores off northwest Africa: sea-surface temperature history over the last 80 ka. *Paleoceanography* 10:661–675